2021

Rheological Analysis of the Mechanical Properties of Murine Lungs Over the Lifespan

Olajumoke Olufunke Harrison
Virginia Commonwealth University

Rheological Analysis of the Mechanical Properties of Murine Lungs Over the Lifespan

A thesis submitted in partial fulfillment of the requirements for the degree of
Master of Science in Biomedical Engineering
at Virginia Commonwealth University

By

Olajumoke Olufunke Harrison
Master's Degree in Biomedical Engineering,
Virginia Commonwealth University 2021
Bachelor's Degree in Biology,
Georgia Southern University 2017

Director: Dr. Rebecca L. Heise,
Associate Professor, Department of Biomedical Engineering

Virginia Commonwealth University
Richmond, Virginia
May, 2021

ACKNOWLEDGEMENT

I would love to thank several people who have inspired me, supported me, uplifted me, and pushed me throughout my master's thesis journey at VCU. I would first like to thank my boyfriend, Moses Douglass III, who was there for me every step of the way. I am forever grateful for the love, support, and push he gave me especially when times were hard. I would like to thank my advisor, Dr. Heise, for allowing me to opportunity to be a part of her lab. With her guidance, I was able to grow into a better researcher. I would like to thank everyone in Dr. Heise's lab, they gave me advice, helped me with my project, and shared great laughs together. Without them my experience at VCU wouldn't have been so fun. Next, I would like to thank my family. Olabisi Akinsanya, Gbenga Harrison Seyi Harrison, Gloria Harrison, Yinka Harrison, Dehinde Harrison, Ola Akinsayna, Abiodun Anifowoshe, Abby Amusa, Destiny Anifowoshe, Andrew Makinde, Bo Amusa, Bolaji Amusa, Amalia Amusa, Khari Amusa, and Zuri Anifowoshe. My biggest and loudest cheerleaders. When time got really hard, I thought of them and became whole. I would like to thank all my friends that were there for me especially, Jada Moodie and Cordell Moodie, I am glad to call you two friends for life. All the time you listen to my worries have paid off. I would like to thank Dr. Arpita Saha, Simpo Akech, and Dr. Christina Voma, who inspired my love for research and supported me to continue onto graduate school. I would love to thank all of Movement Consulting, LLC, they uplifted me in ways I didn't know I needed. I am forever grateful in be in their presence and be a part of something bigger than myself. Lastly, I would to thank all of the rest of the people that made this achievement possible.

TABLE OF CONTENTS

TABLE OF FIGURES

Page

LIST OF ABRREVIATION

AFM	Atomic Force Microscopy
COPD	Chronic Obstructive Pulmonary Disease
ECM	Extracellular Matrix
IPF	Idiopathic pulmonary fibrosis
MMP	Matrix Metalloproteinase
MOM	Middle/Old Mice
PAH	Pulmonary Arterial Hypertension
PBS	Phosphate Buffer Saline
P-V	Pressure-Volume
SOAS	Small Amplitude Shear Oscillation
TIMP	Tissue Inhibitors of Metalloproteinases
WOB	Work of Breathing
YAP	Yes-Associated Protein
YM	Young Mice

Abstract

RHEOLOGICAL ANALYSIS OF THE MECHANICAL PROPERTIES OF MURINE LUNGS OVER THE LIFESPAN

By Olajumoke Olufunke Harrison, M.S.

A thesis submitted in partial fulfillment of the requirements for the degree of Master of Science in Biomedical Engineering at Virginia Commonwealth University

Virginia Commonwealth University, 2021

Major Director: Dr. Rebecca L. Heise, Associate Professor, Department of Biomedical Engineering

To study the effects of aging in murine lungs, we characterized C57Bl6j mice from neonatal to 24-month-old mice. Samples were divided into two groups: Young Mice (YM) and Middle Age/Old Age Mice (MOM). The YM group included the neonatal and 6-10week. The MOM group included 7- and 22–24-month-old mice. Rheological testing was performed using a TA Instruments DHR-2 Rheometer to collect the mechanics of each mice sample. Utilizing a 20-mm

parallel plate fixture, a gap of 0.8-1.0-mm, and a temperature setting of 25C, we conducted a frequency sweep. Samples were the decellularized over a four-day process then lyophilized for mass spectrometry. Histology was also conducted to visualize the structure of the lung. Our results showed that as the age of the mice increased the YM and MOM group, showed an increase in the storage and loss modulus. These results showcase that there are some changes in tissues mechanics that are age-related and this change can be related to decreased lung function.

Vita

Olajumoke Olufunke Harrison was born April 18, 1995, Brooklyn, New York. She graduated from Grayson High School, Loganville, Georgia in 2013. She received her Bachelor's degree in Biology from Georgia Southern University in 2017.She received a Master's of Science in Biomedical Engineering from Virginia Commonwealth University in 2021.

A. INTRODUCTION

1.1 Lung Development

The development of the lungs happens in three main periods: the embryonic, fetal, and postnatal period. The embryonic stage of lungs happens at week 4-7 post conception. This is when the anlage of the right and left lungs presents as two independent outpouchings of the ventral wall of the primitive foregut. Both of these buds will begin to elongate and create a cycle of growth in the mesenchyme and branching. The joining of the laryngotracheal sulci of the lateral walls of the foregut begins then the primitive foregut will be divided into the esophagus and trachea. During the weeks between 5-7 post-conception the lungs are going through the pseudoglandular stage. This is when the formation for the bronchial tree begins. The outgrowth of the terminal bud which leads to the surrounding mesenchyme and the branching of the future airways. The first 20 future airways are formed, and a couple of generations of the alveolar ducts are already present. In addition, the formation of epithelial sprouts begins in the walls of the trachea and bronchi. The canalicular stage is during the 16–26-week post conception. The differentiation of the epithelia will allow the morphological distinction between conducting and respiratory airways. At the 24–38-week post-conception, the saccular stage begins. The branching morphogenesis stops, but alveolarization has not started. The terminal airways are growing in length and in width. Due to the enlargement of the future gas exchange region causes condensation of the mesenchyme. From week 36 to year 3 is the classical alveolarization. During this time, new septa will be lifted off immature preexisting septal and divide the existing airspace. After, the septum rises up to its full height and the first alveoli are formed (Schittny, 2017).

For mice, the lung development is similar, but happens at a much faster rate. The embryonic stage happens at the 9.5-12.5 days after conception. The pseudoglandular stage happens at the 10.5-16.5 days after conception. The canalicular stage happens at 16.5-17.5 days. Saccular stage will begin at the 17.5 days to 5 days after postnatal. The alveolar stage will begin 5 to 30 days postnatal (Shi et al., 2007).

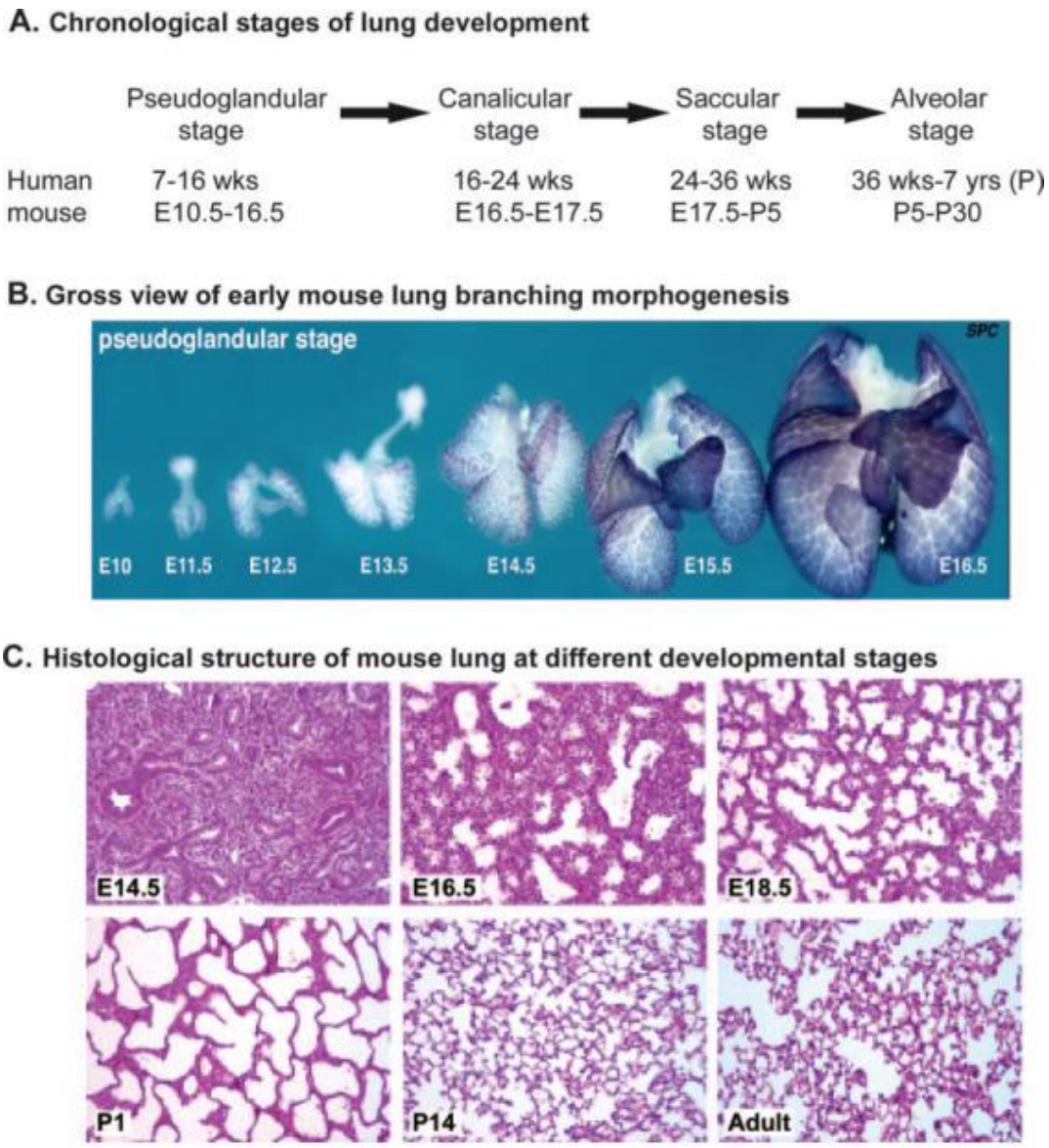

Figure 1. Section A displays the timing of lung development in humans and in mice. The human gestational stages are presented in weeks and the mouse embryonic stages are presented in days.

Section B shows a wide view of a developmental series of early embryonic branching morphogenesis in mice. Section C presented the histological structures using a hematoxylin eosin–stain of the mouse developing lung at different stages(Shi et al., 2007). Produced from Shi et al., 2007 with permission.

1.2 Lung Aging

The structure of the thoracic cavity protects the lungs and is optimal for lung function. Due to aging, changes to the spine, muscles, and ribs overtime will affect normal lung function. As people age the curvature of the spine will decrease the space between the ribs and creates a smaller chest cavity. In addition, there will be changes in the function of the muscles with age. There will be a reduction in inspiratory and expiratory respiratory muscle strength. The decline of respiratory muscle can lead to the inability to ventilate when the demand increases. The physiological aging that happens to the lung is dilation of alveoli, enlargement of airspaces, decreased exchange surface area, and loss of support for peripheral airways. These changes will cause the static elastic recoil of the lung to decrease and the residual volume and functional residual capacity of the lung to increase. The chest will reduce in compliance which will increase the work it takes for a subject to breathe. Various morphological and tissue parameters of lungs will change due to aging. After 30, there is a 1% decline per year in respiratory mechanics and lungs. Between ages 50 to 80 years of age, lung tissue will become about 7% stiffer (Lai-Fook & Hyatt, 2000). Muscle function will decrease by 2%. The mechanical properties of the lung demonstrate a tensegrity dynamic that displays a balance of physical forces, stress, and strain which aids in determining the lung function and structure (Hsia, 2017). In addition, the lungs are constantly experiencing large cyclic mechanical stress and deformation with breath as well as cardiac contraction. Variations of the elastic properties located in the lung linked with aging are crucial in determining lung function (Sicard et al., 2018).

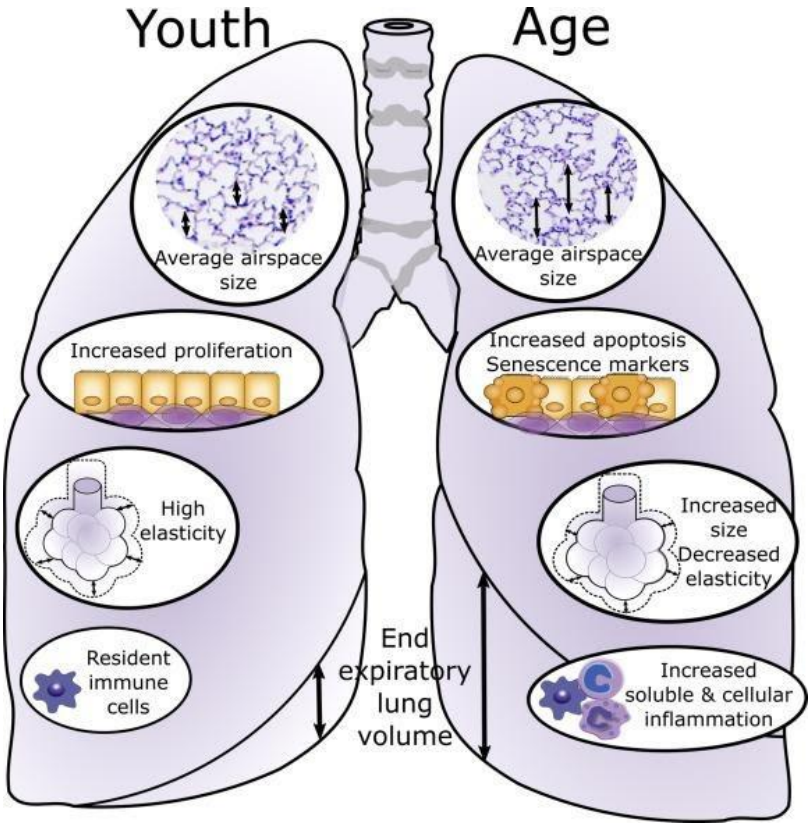

Figure 2 Displays the physiologic changes that happen in the ageing lung. On the left side, presents the young lung which has average airspace size, increased proliferation, high elasticity. The aged lung on the right side shows that the average airspace size will increase as well as increase apoptosis and senescence markers. Elasticity will decrease and increase cellular inflammation (Bowdish, 2019). Produced from Bowdish, 2019 with permission.

1.3 Extracellular Matrix

The lung's extracellular matrix (ECM) is key in providing a scaffold for the cells and contributes to respiratory function's mechanical properties. ECM is critical in the regulation of developmental organogenesis, homeostasis, and injury-repair responses. The cells that reside in the ECM regulate the production and deposition of the ECM throughout development. Through biochemical and biomechanical cues, the ECM regulates diverse cell function, fate, and phenotype. The lung is very heterogeneous depending on location and developmental stage. The composition of the lung ECM changes throughout the developmental stage, making the fetal, neonatal, young, and old adult tissue distinct.

1.4 Composition of the ECM

The core structural components of the entire mammalian ECM include around 300 proteins. The major components are collagens, elastic fibers, proteoglycans, fibronectin, and tenascin. Collagen is composed of three polypeptide alpha chains that form a triple helix structure. These molecules are rod-like in shape and rigid, with a length of about 300nm and a 1.5nm diameter(Kulkarni et al., 2016). The fibrillar collagens (types I,II,III,V, and XI) contribute to the architecture of the lung due to its great tensile strength and low elasticity. In the interstitium of the lung parenchyma contains a majority of type I and III collagen and elastin. The primary component of elastin fibers is elastin. Elastin is an insoluble polymer of the monomeric soluble precursor, tropoelastin. They are mixed with collagen and contribute to the lung's compliance and elastic recoil properties due to its low tensile strength and high elasticity. They provide the structural framework for the alveolar wall. Laminin, is known to be a key component of basement membrane. Laminin is abundant in the developing lungs and plays

crucial roles throughout lung morphogenesis process which includes alveolar growth by supporting cell growth and interaction, specifically, alveolar capillary network formation and remodeling (Luo et al., 2018). Proteoglycans are macromolecules composed of a protein core and glycosaminoglycan side chains. Their function is to maintain the assembly of collagen fibrils, water balance, cell adhesion, and migration. Tenascin and fibronectin are responsible for regulating important cell properties, inflammatory cell chemotaxis and ongoing tissue injury (Suki et al., 2005).

1.5 Changes in Lung ECM with Disease

As the lung ages, the areas of function and structure become weakened to injuries due to different environmental toxins. Environmental toxins can include: airborne aerosols, cigarette smoke, and air pollution. The lung is lined with antioxidant defenses known as the epithelial lining fluid. The fluid is derived from plasma exudate and secretion from resident immune cells. The fluid lining helps to protect the lungs from inhaled pollutants. However, as we age these defenses are reduced, which increases the susceptibility of older people. In this section, we discuss the ECM changes in the developmental and progression of lung such as Asthma, COPD, Idiopathic Pulmonary Fibrosis, Lung Cancer, and Pulmonary Arterial Hypertension.

1.5.1 Asthma

The airway smooth muscle (ASM) is crucial in controlling airway caliber, and structural alterations. The ASM can also be the basis of the airways hyperresponsiveness known as Asthma. The thickened ASM layer in asthma patients also includes ECM components. These

ECM components are important in determining the mechanical properties of the ASM. The ECM is also responsible for transferring force between ASM cells and the ASM to the surrounding tissues. The exposure of serum to ASM cells from patients with Asthma has shown to produce increased levels of ECM proteins. The ECM proteins will then in return affect the proliferation and secretory state of the ASM. Abnormal ECM composition within the ASM can also impact its contractile properties. The remodeling of the ECM in Asthma is determined by the rate of the ongoing deposition and degradation of coll0agen I,II, V, fibronectin, tenascin, lumican, and biglycan. These components may be present due to the activation of fibroblast and myofibroblast. With patients with fatal Asthma, levels of fibronectin and elastic fibers are increased in the smooth muscle of the airways; increases of lumican and biglycan in the airway's matrix structure correlate with tissue injury and worsening lung function(Araujo et al., 2008).

1.5.2 COPD

Chronic Obstructive Pulmonary Disease (COPD) is known as the chronic inflammatory lung disease that causes obstructed airflow from the lungs. This airflow limitation is caused by small airway remodeling leading to the thickening of the airway walls, the loss of the small airways and the engagement of the respiratory air spaces in the alveoli. The structural changes that begin to happen in the ECM cause a biomechanical change that led to a loss of elastic recoil of the lung. This recoil lost suggests that the elastin, a component of the ECM, is the primary target for decomposition. In addition, studies have shown that within the alveolar wall collagen remodeling can contribute to structural changes. Compared to healthy subjects, people with moderate COPD showed alterations in elastic fibers, fibronectin, collagens, tenascin-C and versican in all lung compartments(Annoni et al., 2012)

1.5.3 Idiopathic Pulmonary Fibrosis

Pulmonary fibrosis is characterized as the lung disease that occurs when lung tissue becomes damaged and scarred. The thickening and stiffening of the lung tissue makes it more difficult to breathe. One of the critical features of fibrotic tissue is an increase in its elastic modulus. Increased elastic modulus means that the ECM is becoming stiffer. The mechanotransduction of ECM stiffness plays a critical role in the proliferation, differentiation, and migration of cells. One of the mechanisms of mechanotransduction operates through the Hippo pathway effector YAP. The increased ECM stiffness can drive fibroblast ECM production in a YAP-dependent manner and the expression of YAP has been identified in fibrosis of the lungs. The composition changes due to collagen and elastin deposition in the ECM surrounding the myofibroblast(Herrera et al., n.d.).

1.5.4 Lung Cancer

Lung cancer is the multistep process involving sustained proliferation, evasion of growth suppression, death resistance, inflammatory processes and replicative immortality. During lung cancer, the ECM is a regulator of the cellular responses that underlie cancer markers. Small cell lung cancers will be surrounded by extensive stroma of ECM, this is because it harbors high amounts of fibronectin, laminin, collagen IV and tenascin-C. This remodeling of tumor stroma strongly impacts tissue stiffness. Collagen metabolism will also be a key player in the stiffening of the tumor stroma because it is the main factor of tensile strength. The increase of the stiffness of the stroma leads to the likeliness of tumor cell invasion and metastasis. In addition, the tumor ECM provides an environment that favors proliferation, metastasis, and the inhibition of apoptosis of tumor cells(Parker & Cox, 2020).

1.5.5 Pulmonary Arterial Hypertension

Pulmonary arterial hypertension is characterized by an increased workload in the right heart ventricle as a result of several processes like genetic predisposition, inflammation, cell proliferation, vasoconstriction and vascular modeling. This increased workload impacts the pulmonary arteries resulting in reduced pulmonary arterial compliance. The three-layer architecture of the arterial wall undergoes remodeling leading to thickening of the intimal, medial, and adventitial. Tenascin-C, an ECM component, has been associated with the progression of PAH. In addition, MMPs play a definite role in remodeling. When studying the pulmonary arterial smooth muscle cell in PAH, it showed an imbalance of MMPs and TIMPs which induced massive crosslinking of the ECM (Herrera et al., n.d.).

1.6 Mechanical Testing

Analyzing the mechanical properties of the lungs over the lifespan is crucial in correlating lung structure, elasticity, and compliance with organ, tissue, and cell-scale behaviors (Mitzner, 2011). Current studies looking into the mechanical properties of the intact lung of different species have used: Uniaxial testing, atomic force microscopy (AFM), and microfluidic system. Rheometry has been shown to be advantageous for encompassing a broader measurement range and closely controlling the testing environment (Bates et al., 1994). Variations of the elastic properties located in the lung linked with aging are crucial in determining lung function (Sicard et al., 2018).

1.6.1 Rheometry

Rheometer is an instrument that measures viscosity and viscoelasticity of fluids, semi-solids, and solids. Viscoelasticity is a property of material that exhibits viscous and elastic characteristics. The overall viscoelasticity of a material contains a certain resistance to deformation which is denoted as the complex modulus(G*). The viscoelastic portions are divided into storage(G') and loss(G'') modulus. The storage and loss moduli in viscoelastic materials are able to measure the stored energy which represents the elastic portion of the material and the energy that is released as heat which represents the vicious portion. The elastic and viscous components are important in defining the mechanical behavior of a material. The time dependent-properties or viscoelasticity of a material is associated with stiffness (Bates et al., 1994). Some limitations of rheometry are that high amounts of sample volume are required which is sometimes not available and materials present an intrinsic storage deformation which will affect the measurement results.

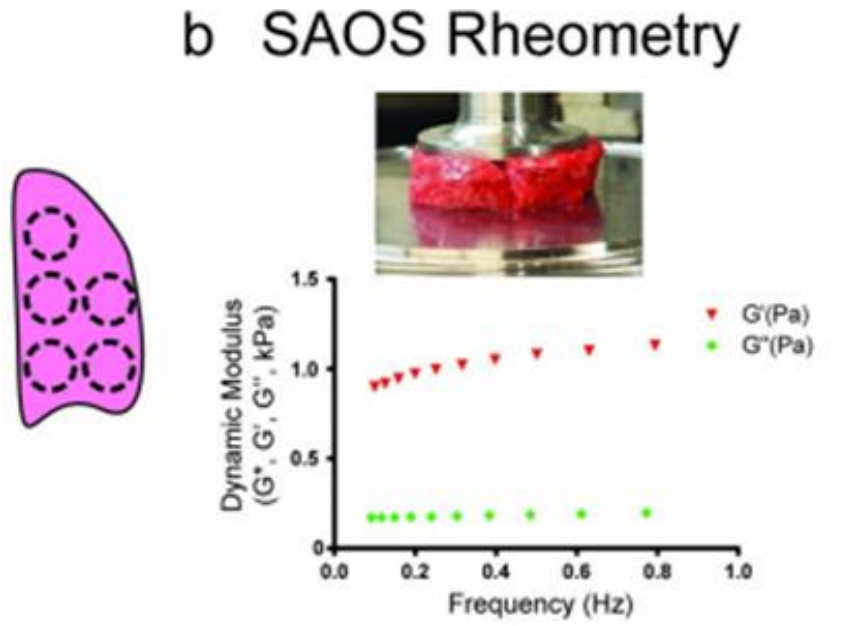

Figure 3. Porcine lungs undergoing a small amplitude shear oscillation rheometry where researchers applied shear across a range of oscillatory frequencies, giving a result of dynamic modulus (Polio et al., 2018). Produced from Polio et al., 2018 with permission.

1.6.2 Atomic Force Microscopy

In previous studies, atomic force microscopy (AFM) was one of the popular tools used to understand lung mechanics. Liu & Tschumperlin's goal was to characterize the variation in tissue stiffness across the anatomical compartments of the airways, vessels, and parenchyma of lung tissue. For testing, lung samples have to be cut into strips. Due to the heterogeneous nature of lung tissue, it is difficult to cut into strips for AFM characterization. To combat heterogeneity extensive preparation needs to be done before testing. The lung structure is stabilized for cutting by inflating the mouse lung with agarose gel. Depending on agarose concentration, the stabilization for cutting varies. Then to isolate the areas of interest for AFM micro indentation, the tissues will have to be visualized by phase contrast microscopy or fluorescence microscopy. In addition, he samples must be attached immediately before AFM measurements are performed because the sample will detach from the coverslip eventually. Smaller samples are less stable and remain in place for a shorter time. The Hertz model assumes that the sample is homogeneity and absolute elastic behavior which we know to be false in lung tissue. Biological materials typically have time-dependent viscoelastic behavior (Liu & Tschumperlin, 2011).

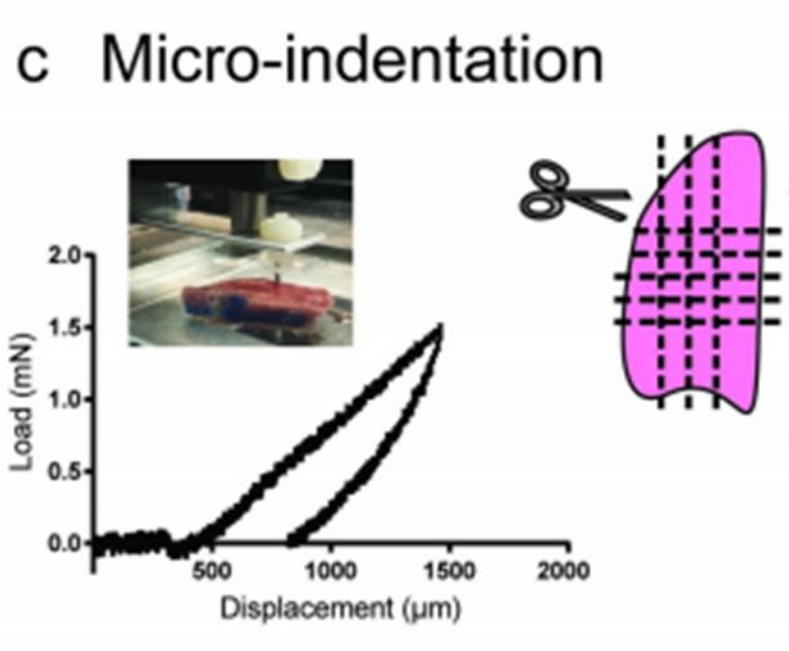

Figure 4 Porcine lungs undergoing atomic force microscopy where researchers applied small compressive forces, which resulted in a force displacement curve, the slope resulting in Young's modulus(Polio et al., 2018). Produced from Polio et al., 2018 with permission.

1.6.3 Uniaxial Testing

Uniaxial testing is a method used to evaluate failure properties of vascular tissue. This tool has been implemented to understand lung tissue mechanics. For testing, lungs have to be subjected to cutting. Samples are usually cut in a dumbbell shape: two shoulders and a gage section in between. Pre-conditioning is conducted by subjecting the tissue to a series of loading and unloading cycles. These pre-conditioning protocols can impact the mechanical response of many biological materials. The shoulders are large making it easy for gripping and the gage section smaller to ensure that the deformation and failure can happen in that area. If unable to cut the dumbbell shape on tissue, the sample is usually cut into a rectangular shape; however, it cannot be assumed that deformation will be uniform throughout the central region. Uniaxial tension does not correlate to the volumetric deformations the lung tissue would be subjected to in reality. Clamping methods are known to influence the stress and strain distribution within the sample. In addition, uniaxial testing cannot provide information about tissue at different temperatures(Griffin et al., 2016).

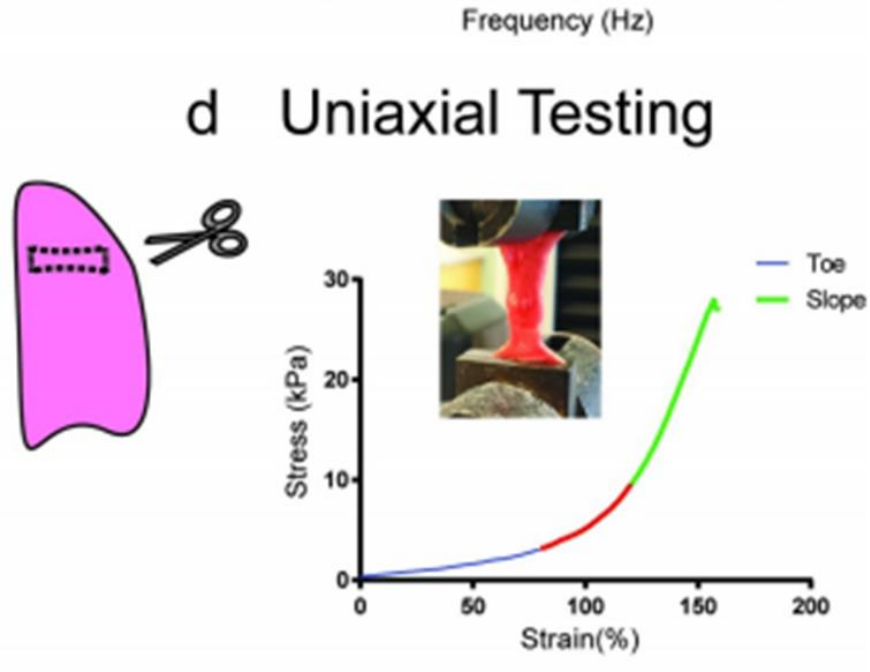

Figure 5. Porcine lungs undergoing uniaxial testing where researchers applied tension to the sample that resulted in a stress-strain curve in which the slope relays a Young's modulus (Polio et al., 2018). Produced from Polio et al., 2018 with permission.

1.6.4 Microfluidic System

A microfluidic chamber consists of three stacked layers each containing a single port and central cavity to contain the lung explant. A rubber gasket to fasten an airtight chamber. To intubate the trachea, a glass microneedle was inserted into the lowermost chamber and the end of it was attached to a syringe pump. In the upper layer, a port was connected to a 0-4 in H2O differential pressure transducer that would continuously measure the pressure within an air bubble that was in the sealed fluid-filled chamber to measure the lung volume. With the microfluidic system they measure compliance through instantaneous pressure-volume curves. However, this method potentially has various sources of error that can be introduced into the system. The lung and reference bubble pressure measurements are highly sensitive. Any physical contact between the lung and explant can alter the deformation of the lung and create inaccurate measurements of lung pressure over time. In addition, the constants that were derived from the calibration runs that are a function of the microfluidic system. These constants would differ depending on chamber size, references bubble volume, and different lung sizes and properties. Any change would require that the system be calibrated for that particular experimental configuration to ensure that the correct P-V curves are collected (Schappell et al., 2020).

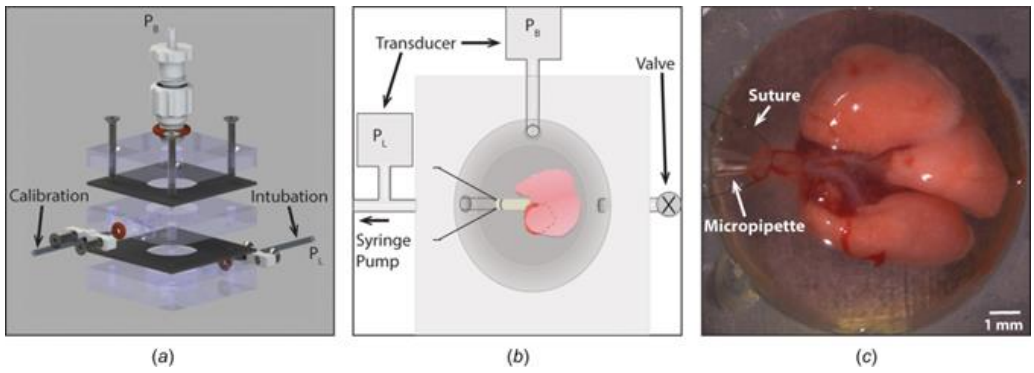

Figure 6. Experimental setup for the measurement of neonatal lung compliance. (Schappell et al., 2020) Produced from Schappell et al., 2020 with permission.

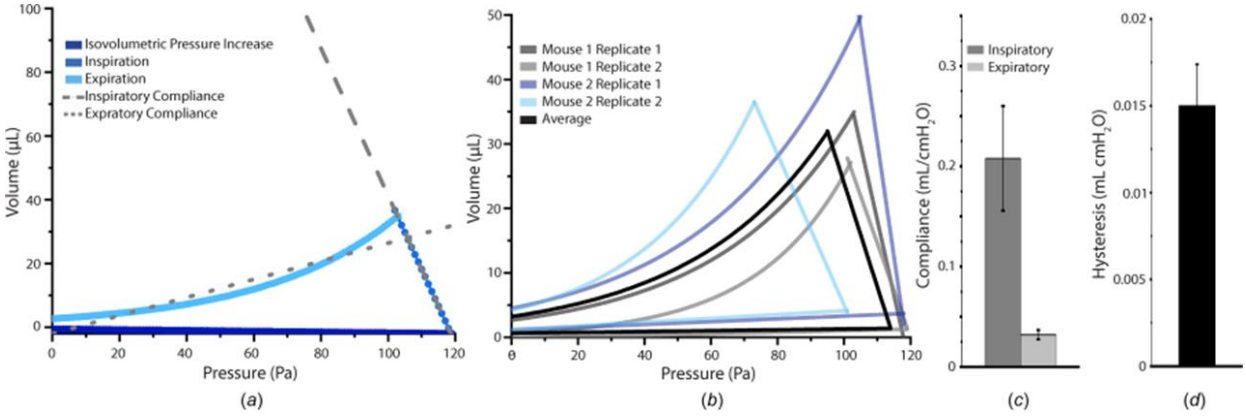

Figure 7. Pressure-Volume curves and the measurements of compliance. (Schappell et al., 2020)**.** Produced from Schappell et al., 2020 with permission.

1.7 Lung Composition Testing

Examining the mechanical properties and composition of the lung is essential in understanding structure and function. The biomechanical properties of connective tissue in the lung play a role in determining how mechanical interactions of the body that produce physical forces will impact its environment at the cellular level. The mechanical forces can directly influence function via cellular signaling during lung development, surfactant release, contractile properties of smooth airway muscle or tissue remodeling. The tissues are composed of cells and the ECM which include biological macromolecules and water. The macromolecules: collagen, elastin, and proteoglycans are essential in determining the mechanical properties of tissue, with collagen being the most abundant. Changes to the individual components of the tissue can be a primary determinant of its mechanical properties which in return helps us understand the complexity of its structure and function (Suki et al., 2005).

1.7.1 Mass Spectrometry

Mass Spectrometry is a tool that determines the mass of large biomolecular complexes, individual biomolecules, small organic molecules, and small atoms with their istropes. Mass spectrometers are capable of separating and detecting ions with high mass resolution and are able to image molecules present at very low concentrations inside the cells. The sensitivity of the instrument can be used to detect biomolecules present in tissue sections. Additionally, mass spectrometers can be used to determine the abundance of a compound in biological samples. They can be implemented in the murine lung tissue aging study. Through analysis, we can see how the abundance of biological compounds change as we age (Chughtai & Heeren, 2010).

1.7.2 Decellularized Lung

The purpose of the decellularization process is to remove cellular components while minimizing the damage to the extracellular matrix. This technique has been used as a material to create tissue engineering applications(Gilbert et al., 2006). In addition, decellularized of tissue can be utilized to study the contributions of ECM components to the mechanical lung properties. We can utilize decellularization to examine the changes that happen to neonatal to old age lungs on the ECM level. There are many different decellularization protocols used to remove the cellular material. They implement physical, chemical, and enzymatic methods to achieve this. Physical methods include freezing, agitation. Enzymatic methods include using DNase and other reagents. Chemical methods use chemical treatments such as sodium chloride, sodium hydroxide, and sodium dodecyl sulfate (SDS)(O'Neill et al., 2013).

1.7.3 Histology

Histology is the microscopic study of cells and tissues through sectioning and staining then examining the interest site under a microscope. There are a variety of ways that histology can be utilized to assess ECM proteins. It can be used to determine the localization of ECM proteins in a tissue as well as assess matrix degradation. In addition, histology can be used as a visual aid to see cellular interaction with ECM proteins (Rosmark et al.,2018).

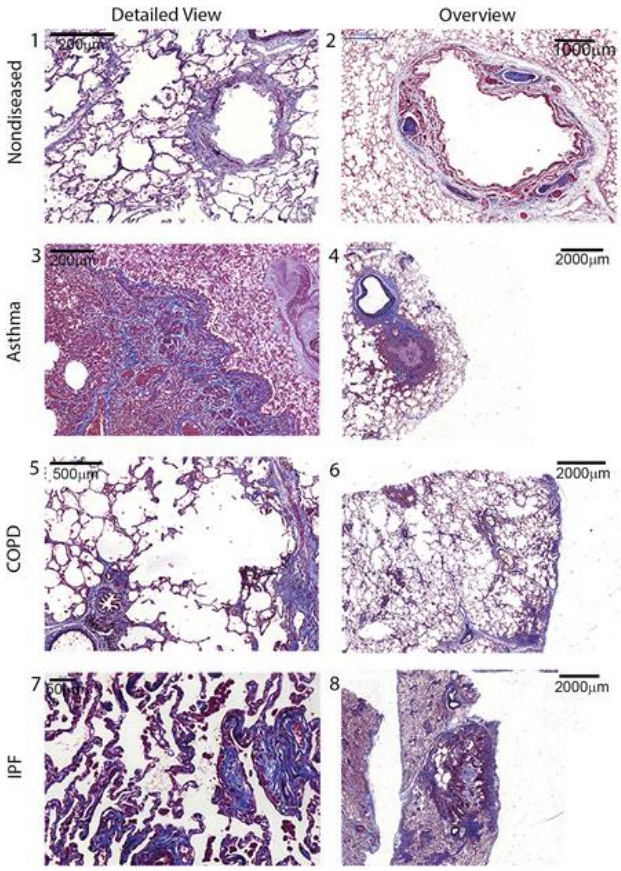

The Journal of Pathology, Volume: 240, Issue: 4, Pages: 397-409, First published: 14 September 2016, DOI: (10.1002/path.4808)

Figure 8. Histological staining showcasing a detailed view and overview nondiseased, Asthma, COPD, and IPF lung tissue ((Burgess et al., 2016). Produced from (Burgess et al., 2016)with permission.

1.8 Objectives of Current Study:

In this study, our goal was to characterize the mechanical properties of the murine lung. We accomplished the goal by using a TA Instruments DHR-2 Rheometer and testing the lungs from neonatal to old age. We used mass spectrometry to quantify the different ECM components that will change as with different age groups. The objective of our study was to analyze the effects of age on rheological lung properties. We hypothesize that the composition of the lung will become stiffer as the mice age causing an increase in the storage and loss modulus. We hypothesize that the mass spectrometry results will show a significant increase in collagen and decease in elastin and laminin production as the age of the mice lung increases.

B. METHODS

2.1 Animals

C57BL6j mice were used in this study under VCU IACUC guidelines. The lungs were collected upon euthanization of C57Bl6j mice (neonatal-24 months old). Lungs were then snap frozen immediately and kept at -80◦C until rheological testing. Murine lungs were categorized into four groups: neonatal (0-10days), young adult (3-6 months), mature/middle adult (10-14 months), and old adult (18-24 months). The age samples were divided into two groups: Young Mice (YM) and Middle Age/Old Age Mice (MOM). The YM group included the neonatal and 6-10week. The MOM group included 7- and 22–24-month-old mice.

2.2 Rheometry

Rheological testing was then performed using a TA Instruments DHR-2 Rheometer with a 20-mm parallel- plate fixture and a gap of 0.8-1.0mm under frequency sweep conditions. The lower Peltier cell was set to 25 C for sample loading as well as after lowering the measuring

system. The system was enclosed within a solvent trap PBS to prevent the lungs from dehydration during testing. The frequency sweeps, had a soak time of 30.0 seconds, 0.5% strain, and angular frequency 0.1 to 100rad/s. All the sweeps were run in triplicate. Cyclic preconditioning was done before every frequency sweep. Samples were stored at -80C.

Figure 9. Schematic of protocol set up for rheological testing.

2.3 Decellularization

After rheological testing, samples were decellularized. Samples were taken out of the -80C fridge and left to defrost. After defrosting, tissue was weighted. One the first day, sample was then cut up into smaller size. Tissue samples were then rinsed three times with 1X PBS. Lastly, they were collected and put into a conical tube and submerge Triton X-100 solution for 24 hours at 4C. For the second day, the samples are taken out of the fridge and rinsed with 1X PBS and cut into finer pieces. Samples are then transferred back into a conical tube and submerged into sodium deoxycholate for 24 hr at 4°C. For the third day, samples are taken out of the 4C fridge and rinsed with 1X PBS and then put back into the conical tube with NaCl solution for 1 hour at 4C. After an hour, samples are taken out and washed with 1X PBS. Tissues are put back into the conical tube filled with a DNase solution for 24hr at 4C. For the fourth day, samples are taken out and rinsed with 1X PBS and then put back into the conical tube with no liquid present. Samples were frozen in -80C until lyophilization (Pouliot et al., 2016).

2.4 Histology

Lungs were fixed with a gravity-assisted flow of 4% paraformaldehyde in the lungs via the trachea at the end of each procedure. Fixed lungs were dehydrated using increasing percentages of ethanol, after being placed in running tap water for 45 minutes, fixed lungs were placed in 50% ethanol overnight, then 70%, 80%, 90%, 95%, and 100% ethanol for 30 minutes each with a repeat of 100% followed by 30 minutes submersion in xylene. The lung tissues were then embedded into paraffin cassettes and 20 lm slices were made with a microtome and transferred onto microscope slides. The slides were then rehydrated and stained with hematoxylin and eosin (H&E) stain. An Vectra Polaris microscope was then used to take color images of the slides with a 20x objective (Kamga Gninzeko et al., 2020)

Services and products in support of the research project were generated by the Virginia Commonwealth University Cancer Mouse Models Core Laboratory, supported, in part, with funding from NIH-NCI Cancer Center Support Grant P30 CA016059.

2.5 Mass Spectrometry

The samples were processed according to a protocol in a paper brought by the investigator. Briefly, the samples were sonicated for 30 minutes and then diluted in 100 mM ammonium bicarbonate. The samples were centrifuged and the supernatant was removed. The samples were reduced with 5 µL of 10 mM dithiothreitol in 0.1 M ammonium bicarbonate at room temperature for 0.5 h. Then they were alkylated with 5 µL 50 mM iodoacetamide in 0.1 M ammonium bicarbonate at room temperature for 0.5 h. The samples were subjected to methanol-chloroform precipitation, and the precipitated protein was resuspended in 50 mM ammonium bicarbonate. The samples were digested with 1 mg trypsin twice overnight and then quenched with 5% (v:v) glacial acetic acid.

The sample was analyzed by a Waters Synapt G2Si mass spectrometer system with a nanospray ion source interfaced to a Waters M-Class C18 reversed-phase capillary column. The peptides were injected onto the trap and analytical columns, and the peptides were eluted from the column by an acetonitrile/0.1% formic acid gradient at a flow rate of 0.4 µL/min over 60 minutes. The nanospray ion source was operated at 3.5 kV. A lockspray compound was used to improve the mass accuracy of the analysis. The digests were analyzed using the double play capability of the instrument acquiring full scan mass spectra at low collision energy to determine peptide molecular weights and product ion spectra at high collision energy to determine amino acid sequence. This mode of analysis produces approximately 10000 CAD spectra of ions ranging in

abundance over several orders of magnitude. Not all CAD spectra are derived from peptides. Each sample was run in triplicate for quantification.

The data were analyzed by database searching using the PLGS search algorithm against the NCBI's mouse database. Quantification was performed using Water's Progenesis quantification program (Kuljanin et al., 2017).

2.6 Statistical Analysis

All murine lung characterization was performed in triplicate. Statistical analysis was performed on the 6-10 week and 22-24-old mice lungs (Figure 13 & 14) with one-way ANOVA. P values of <0.05 were considered significant, p values were $p < 0.001$. We used Graph Prism 9 statistical analysis software

C. RESULTS

Since the lung is both structurally and mechanically heterogeneous tissue, it is difficult to obtain a comprehensive test. To address this, we tried to get five separate lung samples to test for each age group. This gave us a more complete look at the storage and loss modulus of each specific age group (Figures 9-12)**.** Each data set was presented as mean +/- standard deviation.

For figure 9 and 10, the graph displays the results for the storage and loss modulus of the YM group containing the neonatal and 6–10-week group. For the neonatal group, we were able to collect three separate samples and for the 6–10-week group we had a total five samples. In comparing both figure 9 and 10, the storage modulus of YM group is greater than the loss modulus which lets us know that the samples are viscoelastic solids. In figure 9, we see that the 6–10-week-old group had a greater storage modulus than the neonatal group which represents the elastic portion of the sample. In figure 10, we see that the 6–10-week-old group had a greater loss modulus than the neonatal group which represents the vicious portion of the sample. This indicates that the 6–10-week group was able to release more energy as heat and in return is more vicious than the neonatal group. For figure 11, the graph displays the results for the complex modulus of the Ym group. The complex modulus was calculated by dividing the loss modulus (G'') over the storage modulus (G').

For figure 12 and 13, the graph displays the results for the storage modulus of the MOM group containing both the 7 month and 22–24-month-old group. For the 7-month group, we tested two separate samples and the 22–24-month-old group we tested five separate samples. In comparing both figure 12 and 13, the storage modulus of MOM group is greater than the loss modulus which lets us know that the samples are viscoelastic solids. In figure 12, we see that the 22-24-month-old group had a greater storage modulus than the 7-month group. This indicates that the 22-24-month-old group was able to store more energy and in return is more elastic than the 7-

month group. For figure 13, the graph displays the results for the loss modulus of the MOM group containing the 7-month group and 22–24-month-old group. For the 7-month group, we also tested two separate samples and in the tested five separate samples 22–24-month-old group. In figure 13, we see that the 22–24-month-old group had a greater loss modulus than the 7-month group. This indicates that the 22–24-month-old was able to release more energy as heat and in return is more vicious than the 7-month group. For figure 14, the graph displays the results for the complex modulus of the MOM group. The complex modulus was calculated by dividing the loss modulus (G'') over the storage modulus (G').

For figure 13, the graph displays the results for the storage modulus of the 6–10-week group and 22–24-month-old group. The graph displays the 22–24-month group having a higher storage modulus than the 6–10-week group. For figure 14, the graph displays the results for the loss modulus of the 6–10-week group and 22–24-month-old group. The graph displays the 22–24-month group having a higher loss modulus than the 6–10-week group. The 22–24-month-old group had a great storage and loss moduli compared to the 6–10-week group. For figure 18, the graph displays the results for the complex modulus of the MOM group. The complex modulus was calculated by dividing the loss modulus (G'') over the storage modulus (G').

Statistical analysis was conducted on figure 13 and 14 using Graph Prism 9 statistical analysis software. Results showed with one-way ANOVA. P values of <0.05 were considered significant, p values were $p < 0.001$.

In figure 15 and 16 we see histological staining of young mice aged between 8-10 weeks and old mice lungs aged between 20-22 months old using a Vectra Polaris microscope 20x objective. In figure 15, we that the alveolar spaces are mostly uniform and compact. The average spaces also look similar in size. In figure 16, we see that the alveolar spaces are not compact and

are not uniform. The average spaces of the alveolar are much bigger in size compare to the young mice lung in figure 15.

Figure 17, displays a Venn diagram of total individual proteins for neonatal, 6-10 weeks, and 20–24-month aged decell mice lungs. In the middle of the Venn diagram, it represents all of the individual proteins that the neonatal, 6-10 week, and 22–24-month-old group share. We see that these group shared about 431 proteins. We know that the majority of the proteins are similar between the three groups. For the neonatal group, we see that it has 43 individual proteins that are unique. For the 6-10-week-old group, we see that it has 9 individual proteins that are unique. For the 22–24-month-old group, we see that it has 12 induvial proteins that are unique. The neonatal group having the most abundant unique individual proteins that are not shared by any other group.

For figure 18, we see the normalized total spectra for the protein laminin subunit alpha 2. The graph shows that the most is the neonatal group followed by the 6–10-week group and the 22–24-month-old group being the least abundant. For figure 19, we see the normalized total spectra for the protein collagen alpha 2. The graph shows that the most is the 22–24-month-old group followed by the 6–10-week group and neonatal group being the least abundant. For figure 20, we see the normalized total spectra for the protein for elastin. The graph shows that the most is the neonatal group followed by the 6–10-week group and the 22–24-month-old group being the least abundant where it displays no elastin.

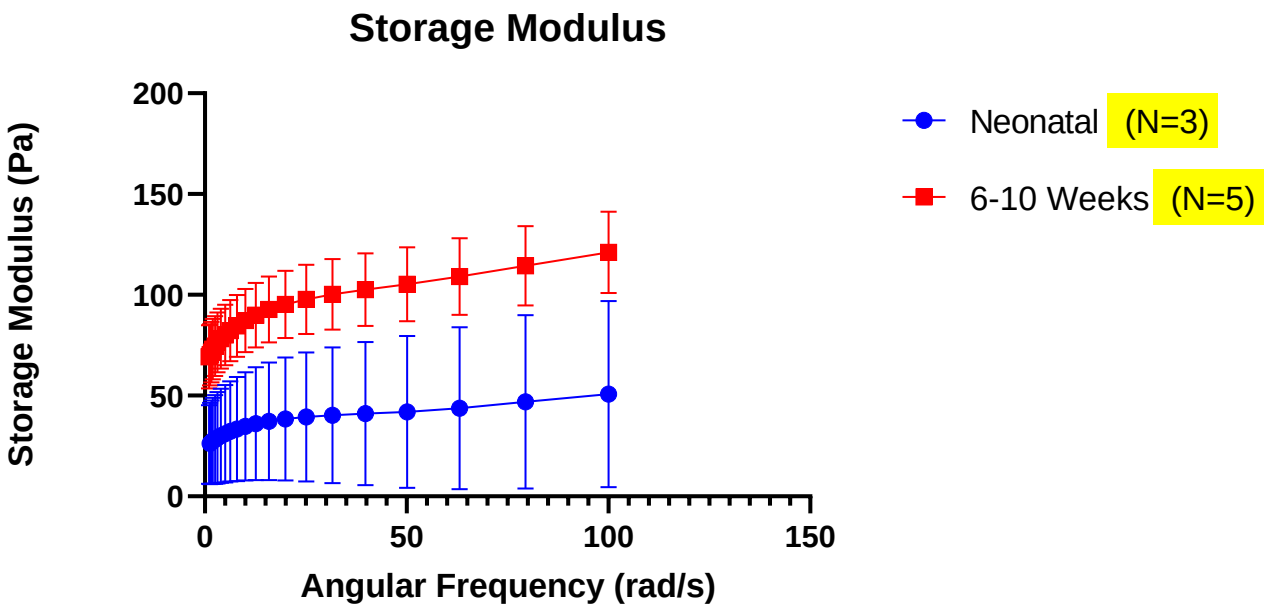

Figure 10: Storage Modulus of YM group: neonatal(N=3) and 6–10-week(N=5) mice. Data are presented as mean +/- standard deviation.

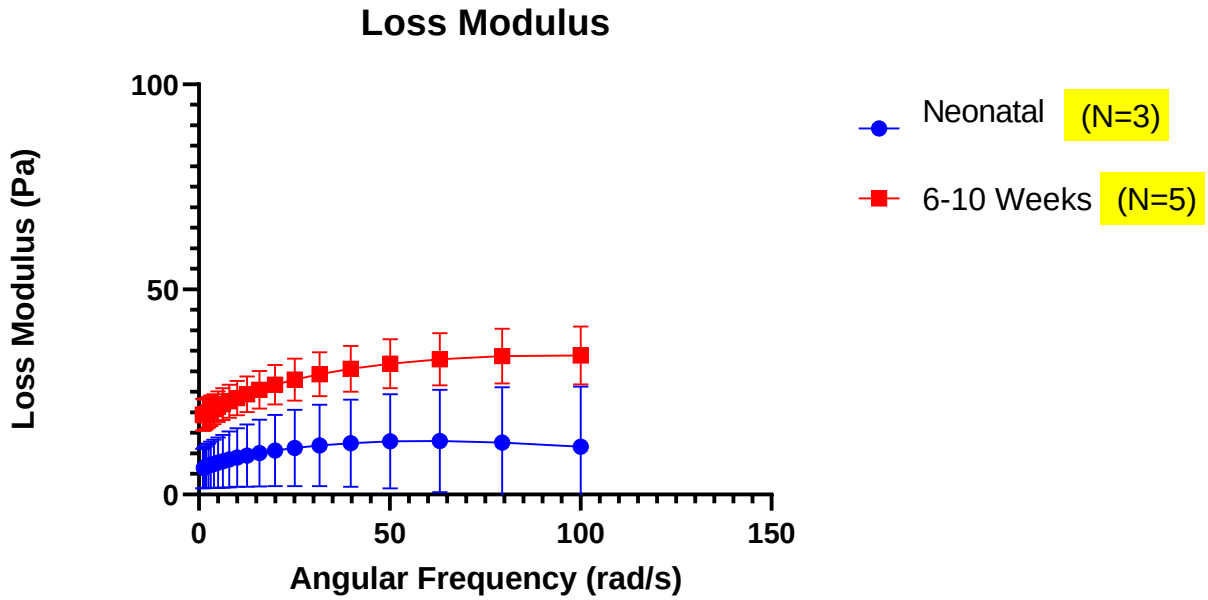

Figure 11: Loss Modulus of YM group: neonatal(N=3) and 6–10-week (N=5) mice. Data are presented as mean +/- standard deviation.

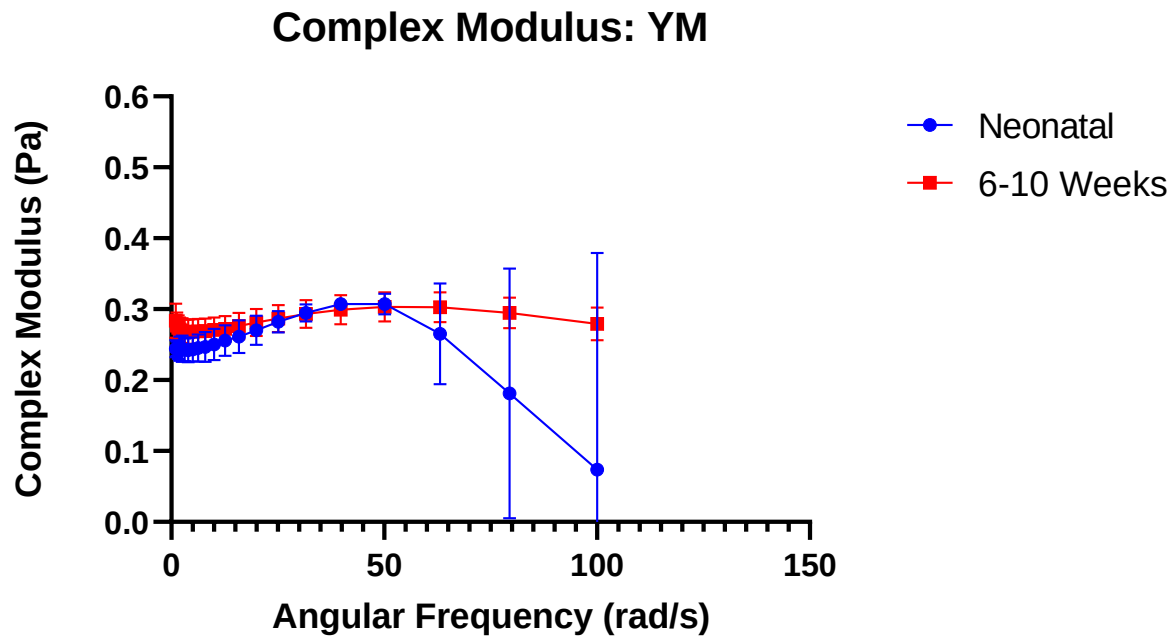

Figure 12: Complex Modulus of YM group: neonatal(N=3) and 6–10-week (N=5) mice. Data are presented as mean +/- standard deviation.

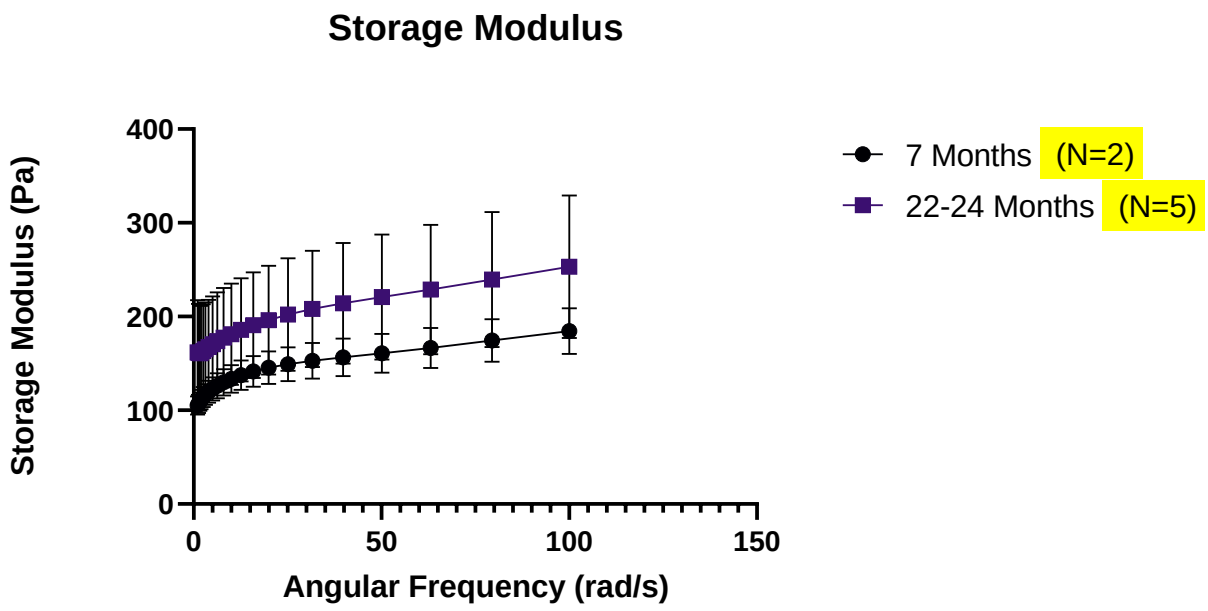

Figure 13: Storage Modulus of MOM group: 7(N=2) and 22–24-month-old(N=5) mice. Data are presented as mean +/- standard deviation.

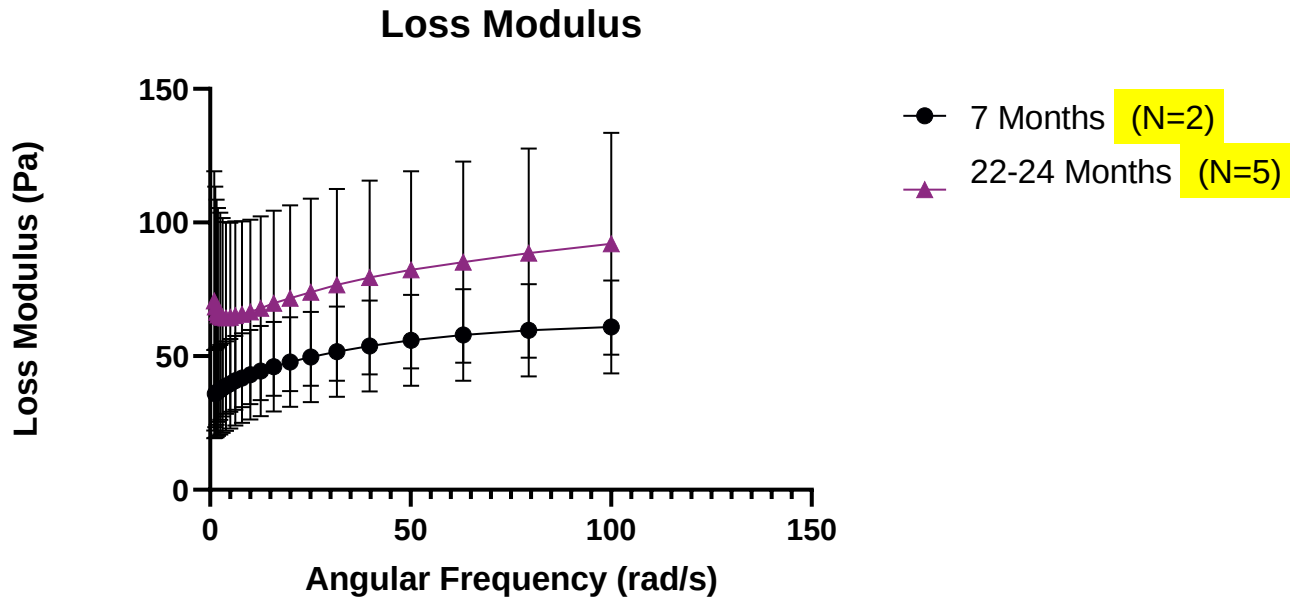

Figure 14: Loss Modulus of MOM group: 7(N=2) and 22–24-month-old(N=5) mice.Data are presented as mean +/- standard deviation.

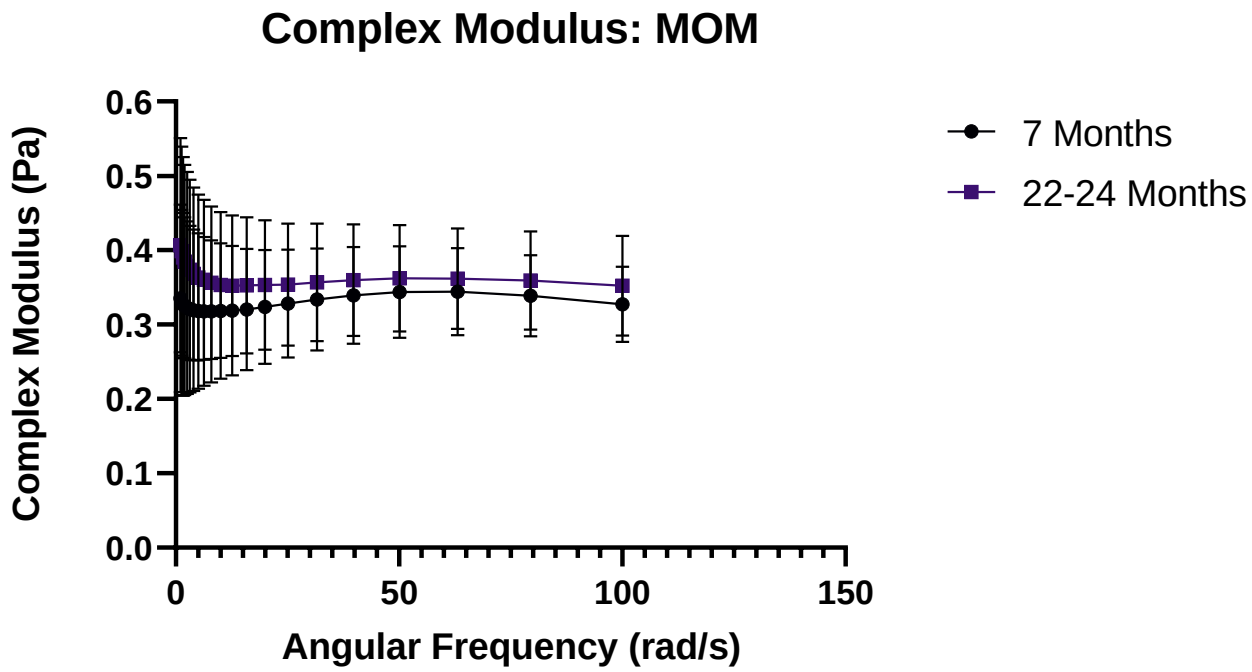

Figure 15: Complex Modulus of MOM group: 7(N=2) and 22–24-month-old(N=5) mice. Data are presented as mean +/- standard deviation.

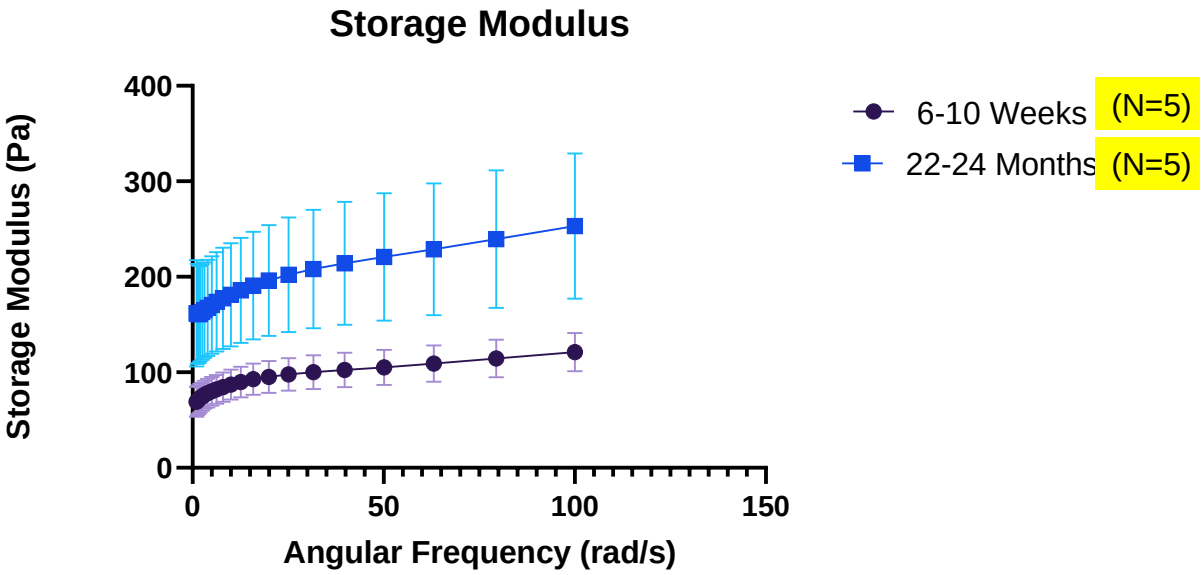

Figure 16. Storage Modulus for 6–10-week-old (N=5) and 22–24-month-old mice(N=5). Data are presented as mean +/- standard deviation.

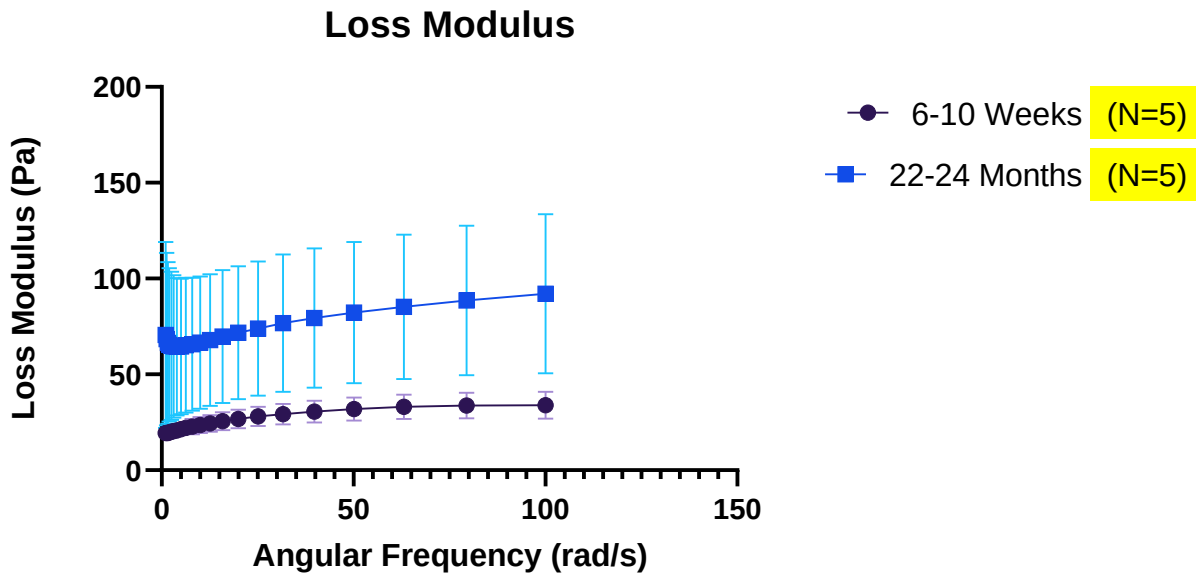

Figure 17. Loss Modulus for 6–10-week-old(N=5) and 22–24-month-old mice(N=5). Data are presented as mean +/- standard deviation.

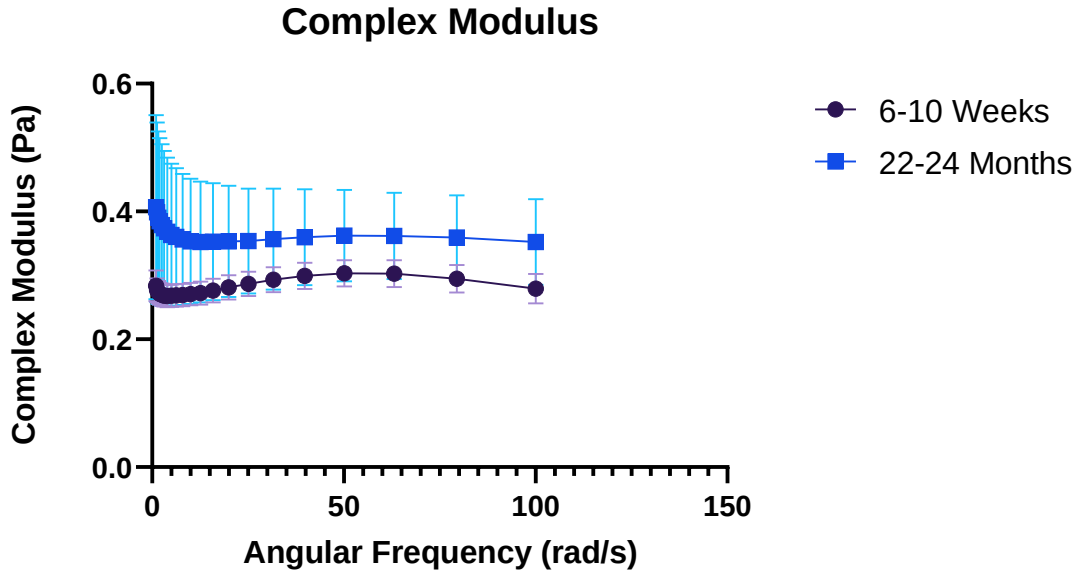

Figure 18: Complex Modulus: 6-10 week mice (N=5) and 22–24-month-old(N=5) mice. Data are presented as mean +/- standard deviation

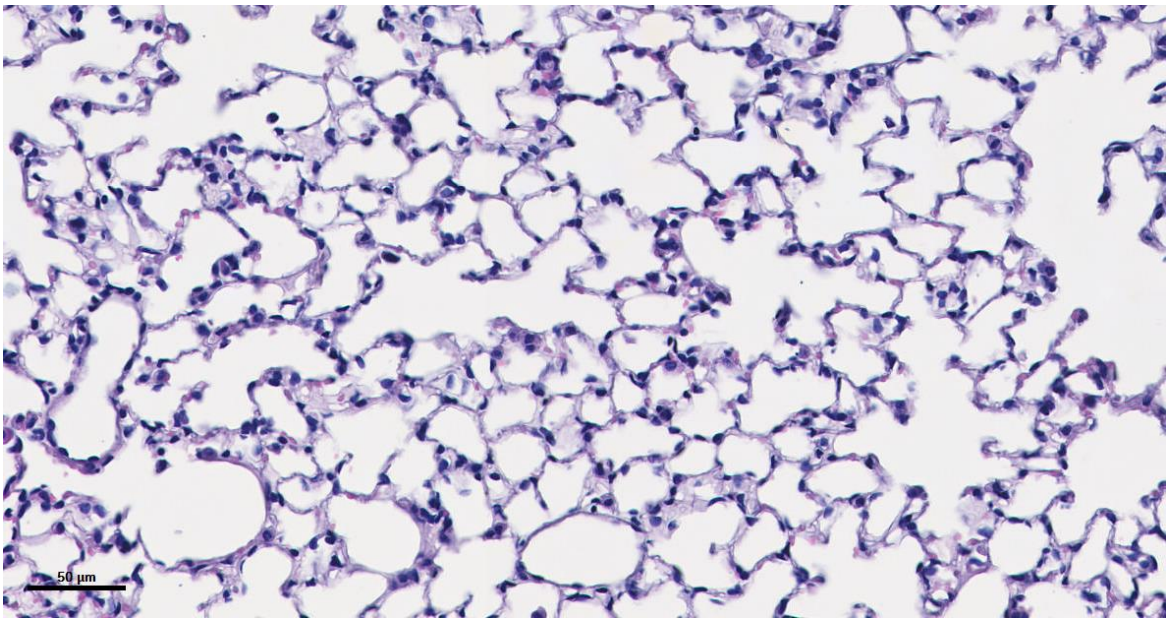

Figure 19. Displays histology image of young mice lungs (8-10weeks old).

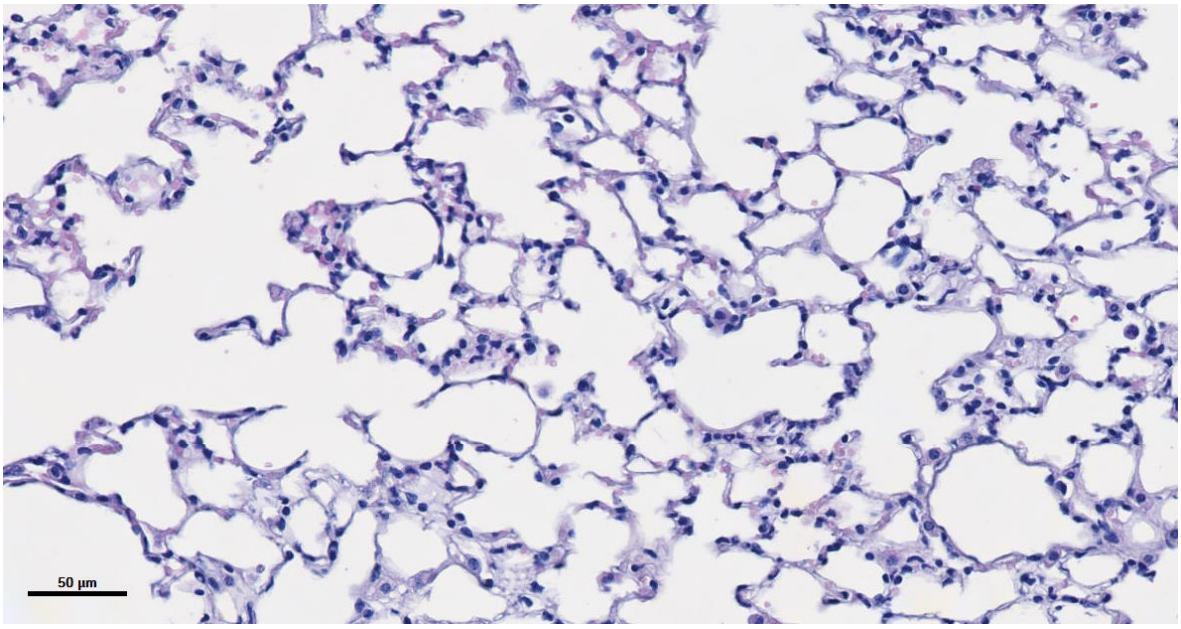

Figure 20. Displays histology image of old mice lungs (20–22-month-old).

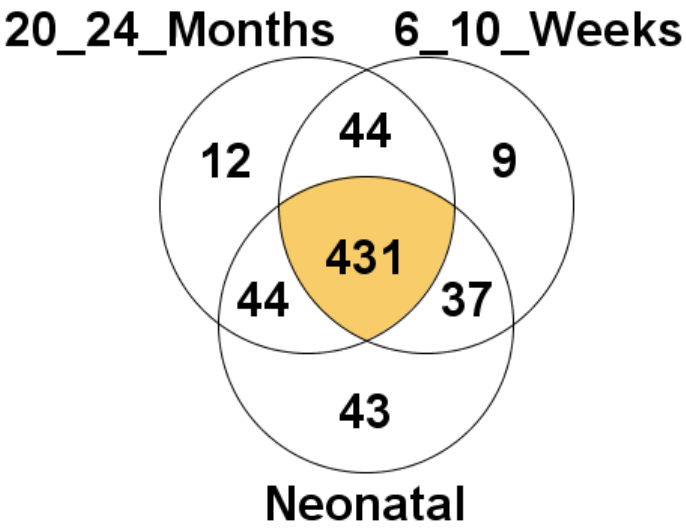

Figure 21. Shows the total individual proteins for neonatal, 6-10 weeks, and 20-24 months age decell mice lungs.

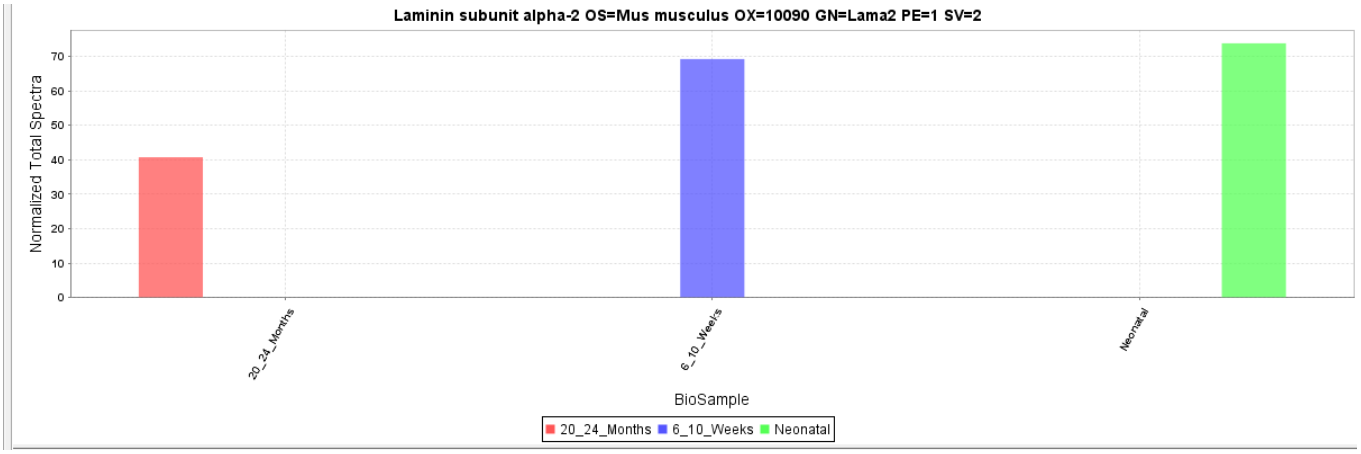

Figure 22. Shows the normalized total spectra of the protein laminin subunit alpha 2 for neonatal, 6-10 weeks, and 20-24 months age mice lungs.

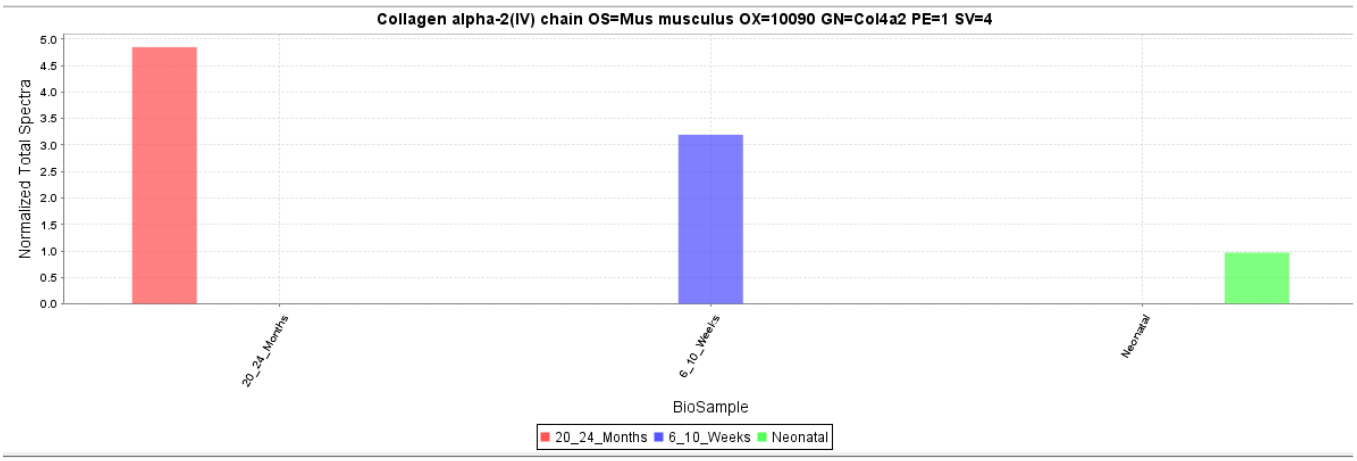

Figure 23. Shows the normalized total spectra of the protein collagen alpha 2 for neonatal, 6-10 weeks, and 20-24 months age mice lungs.

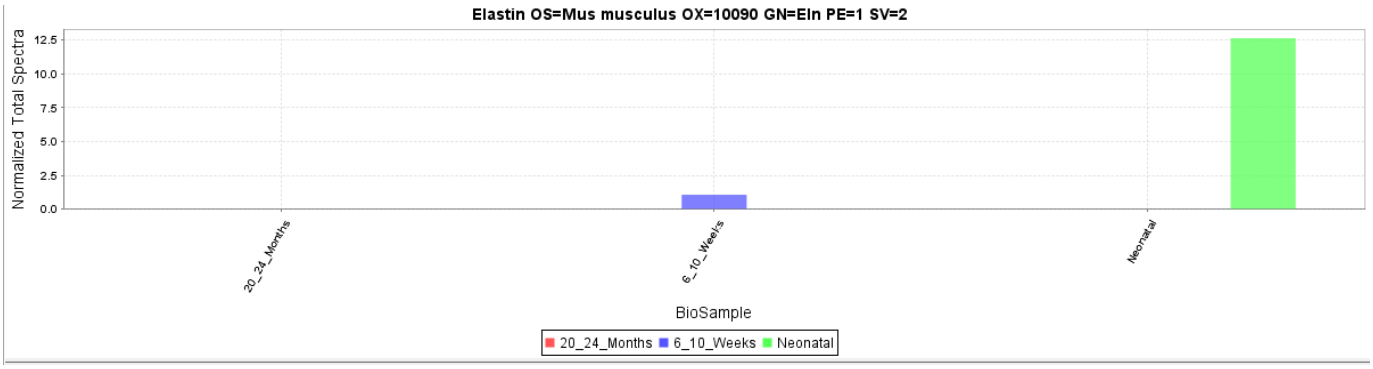

Figure 24. Shows the normalized total spectra of the protein elastin for neonatal, 6-10 weeks, and 20-24 months age mice lungs.

D. DISCUSSION

There has been significant research performed to understand lung mechanics. Especially in neonatal lung mechanics, which is still wildly unknown. Decreased lung function is a common occurrence that happens as we age. This decrease is linked to the structural changes that take place on the macro and micro level of the lung. Lung tissue that aids in keeping airways open can lose elasticity as its ages, resulting in smaller and stiffer lung tissue (Hsia, 2017). We have developed a method using the TA Instruments DHR-2 Rheometer to measure murine lung mechanics from neonatal to old age. By applying a frequency sweep to murine lungs, we were able to gather the data of the lung's storage and loss modulus. Our approach of using a rheometer overcomes challenges seen in other methods used to apply mechanical loads. We were able to use this method for large and small lung tissue. Further, as this method is based on measuring the loss and storage modulus, we are able to link structural changes with age. This study contributes to our understanding of how age takes a crucial part in murine lung tissue mechanics.

Even though our understanding of the roles that the different ECM components play within the structure is limited, we know that the assembly of the ECM is crucial in providing unique tissue-specific microenvironments. Various parts of the ECM are constantly being remodeled and subjected to post-transcriptional changes. The stiffness of the ECM is correlated with the biomechanical properties of the tissue changing. These changes to levels and ratios of the proteins that make up the ECM will have an impact on ECM stiffness. The stiffening of the ECM in response to aging affects cell adhesion and migration (Sicard et al., 2018). Work of breathing (WOB) will also be impacted due to ECM stiffness. WOB is defined as the energy required to inhale oxygen and exhale carbon dioxide. WOB is dependent on the ventilation associated with a given effort and the mechanical efficiency of the chest wall (Aghasafari et al., 2019). In older

patients, there is a decrease in compliance of the alveolar sacs and increase rigidity of the chest wall which would mean that WOB would increase.

For the YM group, the results of the storage modulus of the neonatal and 6–10-week group was always greater than the loss modulus. This indicated to us that our lungs in this group were more elastic than viscous. We also found that the 6–10-week group had a higher storage and loss modulus than the neonatal group. This indicated that the increase in storage and loss modulus from neonatal to 6-10 weeks meant that the structural components of the lung were becoming stiffer as they aged.

For the MOM group, the results of the storage modulus for the 7 and 22-24-month group was always greater than that of the loss modulus group. This also let us know that the lungs were more elastic than vicious. There was an increase from the 7-month group to the 22-24month group. This indicated that the lungs were having an increase in stiffness as we went up in age.

Complex modulus was calculated for all groups. The complex modulus is useful in quantifying the direct measure of the rigidity of a material's structure when it is exposed to stresses below the yield stress. For that reason, the complex modulus is a good indicator of stiffness of a material. For the YM group and MOM group, this study showed a similar trend previous study done with different human lung compartments which also displayed an increase in Young's modulus as age increased (Polio et al., 2018).

The biomechanical properties of lung are composed of cells and the ECM. These biomechanical properties are important in determining how mechanical interactions of the body with its environment will produce physical forces at the cellular level (Suki et al., 2005). These components contain water and different biological macromolecules. The macromolecules that are crucial in determining the biomechanical properties are collagen, elastin, laminin, and

proteoglycans. The most critical macromolecule for structural integrity is collagen. They provide the structural framework for the alveolar wall and are organized to form an axial fiber network extending down from the central airways to the alveolar ducts. Research has shown that collagen prediction will increase in normal aging murine lungs (Mays et al., 1989). Results from this study displayed similar findings where we saw in Figure 23. Our mass spectrometry results showed that as the age of the decellularized lung tissue increased the amount of collagen fragments present also increased. Increased collagen present in the lung is associated with increased crosslinking of collagen fibers. The increased crosslinking leads to reduced compliance and ECM stiffness (Suki & Bartolák-Suki, 2015). Elastin fibers' role in lung elasticity is still wildly unknown. However, the diameter and length of elastin is similar to the distribution of collagen fiber which displays its structural heterogeneity and are mechanically connected to collagen. Past research has shown that elastin plays a big role in lung elasticity at normal breathing lung volumes (Suki & Bartolák-Suki, 2015). Decreased elastin production in the lung is associated with elastic recoil pressure. Results from this study displayed similar findings where we saw in Figure 24. Our mass spectrometry results showed that as the age of the decellularized lung tissue increased the amount of elastin fibers present decreases. Laminin are known as trimeric ECM that are important in the development of the lung tissue. There is still little known about laminin roles in aging. However, in pervious studies observed that ECM gene expression in native lung showed age-related decrease in laminin the old murine lungs compare to the young murine lungs (Godin et al., 2016). Results from this study displayed similar findings where we saw in Figure 22. Our mass spectrometry showed that as age increased the amount of laminin present will decreased. Proteoglycans are the hydrated gels that collagen elastin fibers are embedded in. The composition and ration of the matrix gel will vary amongst different age stages. One critical component of the proteoglycans is the

glycosaminoglycans (GAG), known as a family of highly charged polysaccharides. There are different types of GAGs which molecular weights that vary. Most of the GAGs are linked to a core protein to form proteoglycans. Proteoglycans contribute to the stress-strain components of the ECM. They are responsible for preventing the collapse of the normal lung (Suki et al., 2005).

In a previous study, researchers looked at age-related changes of the human vitreous humor using Rheometry (Tram & Swindle-Reilly,2018). The vitreous humor is located between the lens and retina and occupies 80% of the eye's volume. When we age the vitreous liquefies which compromises its ability to function. This can cause complications such as retinal detachment, muscular holes, and vitreous hemorrhage. The solid phase of the vitreous is known as the cohesive portion of the tissue. The rheological data from the sloid component of the old vitreous samples (ages 65 and above) was significantly higher than the young vitreous samples (65 and below) (Tram & Swindle-Reilly,2018).

In previous studies, a popular technique implemented to visually see the altered change in structure of the lung tissue was histology (Schulte et al., 2019). As we age, the alveoli, small sacs that are responsible for gas exchange, can lose their shape and become baggy. Increased age is associated with lung stiffness and demonstrates a high correlation with increased alveolar wall thickness and decreased lung function. In a previous study, researchers constructed 3D models of young and old human alveolar sacs and fluid-solid interaction was used to investigate the contribution of age-related changes to decline in alveolar sacs function under mechanical ventilation (Aghasafari et al., 2019). Aghasafari and researchers employed pressure-volume loops. Results showed that alveolar sacs were larger in older mice than in young mice. The enlargement of alveolar ducts in older mice models led to a decrease in compliance. This meant that older sacs

would have less tendency to expand compared to younger sacs which indicated stiffening of the tissue (Aghasafari et al., 2019).

The utilization of mass spectrometry to assess residual proteins remaining in decellularized lung allows us to analyze the changes in altered composition of the lung's ECM protein amount over the lifespan. In a previous study, looking to further determine age-related changes in the ECM proteins in mouse lungs found that compared to their young (3-weeks) lungs researchers found that old (1 year) lungs had demonstrated decrease expression of laminin and elastin while having elevated levels collagen (Godin et al., 2016). Our results from the study show a similar trend with the laminin and elastin having decrease expression as we increase in age and increase in collagen when age increases.

Some of the limitations we faced during the study is the varied number of samples per group. Specifically, for the neonatal and 7-month group, we were only able to collect three and two samples in each group. Freezing the sample may have caused some reduction in modulus as shown previously (Polio et al., 2018). After the euthanization of the mice, it is common that the sample is kept frozen to preserve the tissue for testing. However, studies have shown that it is advantageous to test immediately after the collection of the lungs due to freezing the sample causes a reduction in storage and loss modulus. This process is only statistically significant if the samples were frozen in OCT medium or LPN (Polio et al., 2018). However, if the samples were frozen in liquid nitrogen by themselves at -80C, the reduction in loss and storage modulus is not statistically significant. In addition, all samples in this study were treated the same so there would be no particular concern about the reduction in modulus as it should be a uniform reduction across all groups. Mass spectrometry was also done on decellurized samples. During the process of decell, non-proteins like GAGs and polysaccharides of the ECM could have been lost (White et al., 2017).

However, every sample was treated through the same decell protocol so it should be uniform in the loss of some non-proteins.

F. CONCLUSION

This study investigated the age-related changes to the mechanical properties of murine lung using Rheometry. Overall, storage and loss moduli of the old murine lung were found to be larger than those of younger murine lung showcasing that the lungs were getting stiffer overtime. Our mass spectrometry results showed that as aged increased the amount of collagen increased while the amount of laminin and elastin decreased. The results of each group showed a similar trend to previous studies that have been conducted regarding aged related changes. This study is relevant and contributes to our understanding what happens to the mechanical properties of the murine lung and age increases. For a more comprehensive look at the rheological properties of murine and its age-related changes, we hope to gather more samples at different age groups. We would also like to do a comparison of fresh samples and decell samples mass spectrometry to see the difference in abundance of proteins over the lifespan. Additionally, we hope to repeat the study using human lungs.

G. REFERENCES

1. Age-Related Changes in Elastic Fibers and Elastin of Lung | American Review of Respiratory Disease. (n.d.). Retrieved June 9, 2021, from https://www.atsjournals.org/doi/10.1164/arrd.1979.119.3.369?url_ver=Z39.88-2003&rfr_id=ori%3Arid%3Acrossref.org&rfr_dat=cr_pub++0pubmed&
2. Aghasafari, P., Heise, R. L., Reynolds, A., & Pidaparti, R. M. (2019). Aging Effects on Alveolar Sacs Under Mechanical Ventilation. The Journals of Gerontology Series A: Biological Sciences and Medical Sciences, 74(2), 139–146. https://doi.org/10.1093/gerona/gly097
3. Angelidis, I., Simon, L. M., Fernandez, I. E., Strunz, M., Mayr, C. H., Greiffo, F. R., Tsitsiridis, G., Ansari, M., Graf, E., Strom, T.-M., Nagendran, M., Desai, T., Eickelberg, O., Mann, M., Theis, F. J., & Schiller, H. B. (2019). An atlas of the aging lung mapped by single cell transcriptomics and deep tissue proteomics. Nature Communications, 10(1), 963. https://doi.org/10.1038/s41467-019-08831-9
4. Annoni, R., Lanças, T., Tanigawa, R. Y., Matsushita, M. de M., Fernezlian, S. de M., Bruno, A., Silva, L. F. F. da, Roughley, P. J., Battaglia, S., Dolhnikoff, M., Hiemstra, P. S., Sterk, P. J., Rabe, K. F., & Mauad, T. (2012). Extracellular matrix composition in COPD. European Respiratory Journal, 40(6), 1362–1373. https://doi.org/10.1183/09031936.00192611
5. Araujo, B. B., Dolhnikoff, M., Silva, L. F. F., Elliot, J., Lindeman, J. H. N., Ferreira, D. S., Mulder, A., Gomes, H. a. P., Fernezlian, S. M., James, A., & Mauad, T. (2008). Extracellular matrix components and regulators in the airway smooth muscle in asthma. European Respiratory Journal, 32(1), 61–69. https://doi.org/10.1183/09031936.00147807

6. Bates, J. H., Maksym, G. N., Navajas, D., & Suki, B. (1994). Lung tissue rheology and 1/f noise. Annals of Biomedical Engineering, 22(6), 674–681. https://doi.org/10.1007/BF02368292

7. Bottje, W., Wang, S., Kelly, F., Dunster, C., Williams, A., & Mudway, I. (1998). Antioxidant defenses in lung lining fluid of broilers: impact of poor ventilation conditions. Poultry Science, 77(4), 516–522. https://doi.org/10.1093/ps/77.4.516

8. Bowdish, D. M. E. (2019). The Aging Lung: Is Lung Health Good Health for Older Adults? CHEST, 155(2), 391–400. https://doi.org/10.1016/j.chest.2018.09.003

9. Burgess, J. K., Mauad, T., Tjin, G., Karlsson, J. C., & Westergren-Thorsson, G. (2016). The extracellular matrix – the under-recognized element in lung disease? The Journal of Pathology, 240(4), 397–409. https://doi.org/10.1002/path.4808

10. Burgstaller, G., Oehrle, B., Gerckens, M., White, E. S., Schiller, H. B., & Eickelberg, O. (2017). The instructive extracellular matrix of the lung: basic composition and alterations in chronic lung disease. European Respiratory Journal, 50(1), 1601805. https://doi.org/10.1183/13993003.01805-2016

11. Chanda, D., Otoupalova, E., Smith, S. R., Volckaert, T., De Langhe, S. P., & Thannickal, V. J. (2019). Developmental pathways in the pathogenesis of lung fibrosis. Molecular Aspects of Medicine, 65, 56–69. https://doi.org/10.1016/j.mam.2018.08.004

12. Chughtai, K., & Heeren, R. M. A. (2010). Mass Spectrometric Imaging for biomedical tissue analysis. Chemical Reviews, 110(5), 3237–3277. https://doi.org/10.1021/cr100012c

13. de Hilster, R. H. J., Sharma, P. K., Jonker, M. R., White, E. S., Gercama, E. A., Roobeek, M., Timens, W., Harmsen, M. C., Hylkema, M. N., & Burgess, J. K. (2020).

Human lung extracellular matrix hydrogels resemble the stiffness and viscoelasticity of native lung tissue. American Journal of Physiology. Lung Cellular and Molecular Physiology, 318(4), L698–L704. https://doi.org/10.1152/ajplung.00451.2019

14. Determination of rheology and surface tension of airway surface liquid: a review of clinical relevance and measurement techniques | Respiratory Research | Full Text. (n.d.). Retrieved April 10, 2021, from https://respiratory-research.biomedcentral.com/articles/10.1186/s12931-019-1229-1#availability-of-data-and-materials

15. Dynamic properties of lung parenchyma: mechanical contributions of fiber network and interstitial cells | Journal of Applied Physiology. (n.d.). Retrieved April 10, 2021, from https://journals.physiology.org/doi/full/10.1152/jappl.1997.83.5.1420

16. Gilbert, T. W., Sellaro, T. L., & Badylak, S. F. (2006). Decellularization of tissues and organs. Biomaterials, 27(19), 3675–3683. https://doi.org/10.1016/j.biomaterials.2006.02.014

17. Godin, L. M., Sandri, B. J., Wagner, D. E., Meyer, C. M., Price, A. P., Akinnola, I., Weiss, D. J., & Panoskaltsis-Mortari, A. (2016). Decreased Laminin Expression by Human Lung Epithelial Cells and Fibroblasts Cultured in Acellular Lung Scaffolds from Aged Mice. PLOS ONE, 11(3), e0150966. https://doi.org/10.1371/journal.pone.0150966

18. Griffin, M., Premakumar, Y., Seifalian, A., Butler, P. E., & Szarko, M. (2016). Biomechanical Characterization of Human Soft Tissues Using Indentation and Tensile Testing. Journal of Visualized Experiments : JoVE, 118. https://doi.org/10.3791/54872

19. Herrera, J., Forster, C., Pengo, T., Montero, A., Swift, J., Schwartz, M. A., Henke, C. A., & Bitterman, P. B. (2019). Registration of the extracellular matrix components

constituting the fibroblastic focus in idiopathic pulmonary fibrosis. JCI Insight, 4(1). https://doi.org/10.1172/jci.insight.125185

20. Herrera, J., Henke, C. A., & Bitterman, P. B. (n.d.). Extracellular matrix as a driver of progressive fibrosis. The Journal of Clinical Investigation, 128(1), 45–53. https://doi.org/10.1172/JCI93557

21. Hsia, C. C. W. (2017). Comparative analysis of the mechanical signals in lung development and compensatory growth. Cell and Tissue Research, 367(3), 687–705. https://doi.org/10.1007/s00441-016-2558-8

22. Ito, J. T., Lourenço, J. D., Righetti, R. F., Tibério, I. F. L. C., Prado, C. M., & Lopes, F. D. T. Q. S. (2019). Extracellular Matrix Component Remodeling in Respiratory Diseases: What Has Been Found in Clinical and Experimental Studies? Cells, 8(4). https://doi.org/10.3390/cells8040342

23. Janssens, J. P., Pache, J. C., & Nicod, L. P. (1999). Physiological changes in respiratory function associated with ageing. The European Respiratory Journal, 13(1), 197–205. https://doi.org/10.1034/j.1399-3003.1999.13a36.x

24. Kalikkot Thekkeveedu, R., Guaman, M. C., & Shivanna, B. (2017). Bronchopulmonary dysplasia: A review of pathogenesis and pathophysiology. Respiratory Medicine, 132, 170–177. https://doi.org/10.1016/j.rmed.2017.10.014

25. Kamga Gninzeko, F. J., Valentine, M. S., Tho, C. K., Chindal, S. R., Boc, S., Dhapare, S., Momin, M. A. M., Hassan, A., Hindle, M., Farkas, D. R., Longest, P. W., & Heise, R. L. (2020). Excipient Enhanced Growth Aerosol Surfactant Replacement Therapy in an In Vivo Rat Lung Injury Model. Journal of Aerosol Medicine and Pulmonary Drug Delivery, 33(6), 314–322. https://doi.org/10.1089/jamp.2020.1593

26. Kuljanin, M., Brown, C. F. C., Raleigh, M. J., Lajoie, G. A., & Flynn, L. E. (2017). Collagenase treatment enhances proteomic coverage of low-abundance proteins in decellularized matrix bioscaffolds. Biomaterials, 144, 130–143. https://doi.org/10.1016/j.biomaterials.2017.08.012

27. Kulkarni, T., O'Reilly, P., Antony, V. B., Gaggar, A., & Thannickal, V. J. (2016). Matrix Remodeling in Pulmonary Fibrosis and Emphysema. American Journal of Respiratory Cell and Molecular Biology, 54(6), 751–760. https://doi.org/10.1165/rcmb.2015-0166PS

28. Lai-Fook, S. J., & Hyatt, R. E. (2000). Effects of age on elastic moduli of human lungs. Journal of Applied Physiology (Bethesda, Md.: 1985), 89(1), 163–168. https://doi.org/10.1152/jappl.2000.89.1.163

29. Leonard, A. K., Loughran, E. A., Klymenko, Y., Liu, Y., Kim, O., Asem, M., McAbee, K., Ravosa, M. J., & Sharon Stack, M. (2018). Methods for the visualization and analysis of extracellular matrix protein structure and degradation. Methods in Cell Biology, 143, 79–95. https://doi.org/10.1016/bs.mcb.2017.08.005

30. Link, P. A., Pouliot, R. A., Mikhaiel, N. S., Young, B. M., & Heise, R. L. (2017). Tunable Hydrogels from Pulmonary Extracellular Matrix for 3D Cell Culture. JoVE (Journal of Visualized Experiments), 119, e55094. https://doi.org/10.3791/55094

31. Liu, F., & Tschumperlin, D. J. (2011). Micro-Mechanical Characterization of Lung Tissue Using Atomic Force Microscopy. Journal of Visualized Experiments : JoVE, 54. https://doi.org/10.3791/2911

32. Lu, P., Takai, K., Weaver, V. M., & Werb, Z. (2011). Extracellular Matrix Degradation and Remodeling in Development and Disease. Cold Spring Harbor Perspectives in Biology, 3(12), a005058. https://doi.org/10.1101/cshperspect.a005058

33. Lung Development - an overview | ScienceDirect Topics. (n.d.). Retrieved April 10, 2021, from https://www.sciencedirect.com/topics/medicine-and-dentistry/lung-development

34. Luo, Y., Li, N., Chen, H., Fernandez, G. E., Warburton, D., Moats, R., Mecham, R. P., Krenitsky, D., Pryhuber, G. S., & Shi, W. (2018). Spatial and temporal changes in extracellular elastin and laminin distribution during lung alveolar development. Scientific Reports, 8(1), 8334. https://doi.org/10.1038/s41598-018-26673-1

35. Mays, P. K., McAnulty, R. J., & Laurent, G. J. (1989). Age-related changes in lung collagen metabolism. A role for degradation in regulating lung collagen production. The American Review of Respiratory Disease, 140(2), 410–416. https://doi.org/10.1164/ajrccm/140.2.410

36. Miller, K. S., Edelstein, L., Connizzo, B. K., & Soslowsky, L. J. (2012). Effect of Preconditioning and Stress Relaxation on Local Collagen Fiber Re-Alignment: Inhomogeneous Properties of Rat Supraspinatus Tendon. Journal of Biomechanical Engineering, 134(3), 31007-NaN. https://doi.org/10.1115/1.4006340

37. Mitzner, W. (2011). MECHANICS OF THE LUNG IN THE 20TH CENTURY. Comprehensive Physiology, 1(4), 2009–2027. https://doi.org/10.1002/cphy.c100067

38. Morrisey, E. E., & Hogan, B. L. M. (2010). Preparing for the First Breath: Genetic and Cellular Mechanisms in Lung Development. Developmental Cell, 18(1), 8–23. https://doi.org/10.1016/j.devcel.2009.12.010

39. Mullassery, D., & Smith, N. P. (2015). Lung development. Seminars in Pediatric Surgery, 24(4), 152–155. https://doi.org/10.1053/j.sempedsurg.2015.01.011

40. O'Neill, J. D., Anfang, R., Anandappa, A., Costa, J., Javidfar, J., Wobma, H. M., Singh, G., Freytes, D. O., Bacchetta, M. D., Sonett, J. R., & Vunjak-Novakovic, G. (2013). Decellularization of Human and Porcine Lung Tissues for Pulmonary Tissue Engineering. The Annals of Thoracic Surgery, 96(3), 1046–1056. https://doi.org/10.1016/j.athoracsur.2013.04.022

41. Onursal, C., Dick, E., Angelidis, I., Schiller, H. B., & Staab-Weijnitz, C. A. (2021). Collagen Biosynthesis, Processing, and Maturation in Lung Ageing. Frontiers in Medicine, 0. https://doi.org/10.3389/fmed.2021.593874

42. Parker, A. L., & Cox, T. R. (2020). The Role of the ECM in Lung Cancer Dormancy and Outgrowth. Frontiers in Oncology, 10. https://doi.org/10.3389/fonc.2020.01766

43. Petersen, T. H., Calle, E. A., Colehour, M. B., & Niklason, L. E. (2012). Matrix Composition and Mechanics of Decellularized Lung Scaffolds. Cells Tissues Organs, 195(3), 222–231. https://doi.org/10.1159/000324896

44. Polio, S. R., Kundu, A. N., Dougan, C. E., Birch, N. P., Aurian-Blajeni, D. E., Schiffman, J. D., Crosby, A. J., & Peyton, S. R. (2018). Cross-platform mechanical characterization of lung tissue. PLoS ONE, 13(10). https://doi.org/10.1371/journal.pone.0204765

45. Pouliot, R. A., Link, P. A., Mikhaiel, N. S., Schneck, M. B., Valentine, M. S., Gninzeko, F. J. K., Herbert, J. A., Sakagami, M., & Heise, R. L. (2016). Development and characterization of a naturally derived lung extracellular matrix hydrogel. Journal of

Biomedical Materials Research Part A, 104(8), 1922–1935. https://doi.org/https://doi.org/10.1002/jbm.a.35726

46. Rosmark, O., Åhrman, E., Müller, C., Elowsson Rendin, L., Eriksson, L., Malmström, A., Hallgren, O., Larsson-Callerfelt, A.-K., Westergren-Thorsson, G., & Malmström, J. (2018). Quantifying extracellular matrix turnover in human lung scaffold cultures. Scientific Reports, 8(1), 5409. https://doi.org/10.1038/s41598-018-23702-x

47. Rozario, T., & DeSimone, D. W. (2010). The extracellular matrix in development and morphogenesis: A dynamic view. Developmental Biology, 341(1), 126–140. https://doi.org/10.1016/j.ydbio.2009.10.026

48. Schappell, L. E., Minahan, D. J., & Gleghorn, J. P. (2020). A Microfluidic System to Measure Neonatal Lung Compliance Over Late Stage Development as a Functional Measure of Lung Tissue Mechanics. Journal of Biomechanical Engineering, 142(100803). https://doi.org/10.1115/1.4047133

49. Schittny, J. C. (2017). Development of the lung. Cell and Tissue Research, 367(3), 427–444. https://doi.org/10.1007/s00441-016-2545-0

50. Schöneich, C. (2005). Mass spectrometry in aging research. Mass Spectrometry Reviews, 24(5), 701–718. https://doi.org/https://doi.org/10.1002/mas.20035

51. Schulte, H., Mühlfeld, C., & Brandenberger, C. (2019). Age-Related Structural and Functional Changes in the Mouse Lung. Frontiers in Physiology, 10. https://doi.org/10.3389/fphys.2019.01466

52. Sherratt, M. J. (2009). Tissue elasticity and the ageing elastic fibre. Age, 31(4), 305–325. https://doi.org/10.1007/s11357-009-9103-6

53. Shi, W., Bellusci, S., & Warburton, D. (2007). Lung Development and Adult Lung Diseases. CHEST, 132(2), 651–656. https://doi.org/10.1378/chest.06-2663

54. Sicard, D., Haak, A. J., Choi, K. M., Craig, A. R., Fredenburgh, L. E., & Tschumperlin, D. J. (2018). Aging and anatomical variations in lung tissue stiffness. American Journal of Physiology. Lung Cellular and Molecular Physiology, 314(6), L946–L955. https://doi.org/10.1152/ajplung.00415.2017

55. Su, J., Satchell, S. C., Shah, R. N., & Wertheim, J. A. (2018). Kidney Decellularized Extracellular Matrix Hydrogels: Rheological Characterization and Human Glomerular Endothelial Cell Response to Encapsulation. Journal of Biomedical Materials Research. Part A, 106(9), 2448–2462. https://doi.org/10.1002/jbm.a.36439

56. Subramaniam, K., Kumar, H., & Tawhai, M. H. (2017). Evidence for age-dependent air-space enlargement contributing to loss of lung tissue elastic recoil pressure and increased shear modulus in older age. Journal of Applied Physiology, 123(1), 79–87. https://doi.org/10.1152/japplphysiol.00208.2016

57. Suki, B., & Bartolák-Suki, E. (2015). Biomechanics of the Aging Lung Parenchyma. In B. Derby & R. Akhtar (Eds.), Mechanical Properties of Aging Soft Tissues (pp. 95–133). Springer International Publishing. https://doi.org/10.1007/978-3-319-03970-1_5

58. Suki, B., Ito, S., Stamenović, D., Lutchen, K. R., & Ingenito, E. P. (2005a). Biomechanics of the lung parenchyma: critical roles of collagen and mechanical forces. Journal of Applied Physiology, 98(5), 1892–1899. https://doi.org/10.1152/japplphysiol.01087.2004

59. Suki, B., Ito, S., Stamenović, D., Lutchen, K. R., & Ingenito, E. P. (2005b). Biomechanics of the lung parenchyma: critical roles of collagen and mechanical forces.

Journal of Applied Physiology, 98(5), 1892–1899. https://doi.org/10.1152/japplphysiol.01087.2004

60. Tram, N. K., & Swindle-Reilly, K. E. (2018). Rheological Properties and Age-Related Changes of the Human Vitreous Humor. Frontiers in Bioengineering and Biotechnology, 6. https://doi.org/10.3389/fbioe.2018.00199

61. Tschumperlin, D. J. (2015). Matrix, mesenchyme, and mechanotransduction. Annals of the American Thoracic Society, 12 Suppl 1, S24-29. https://doi.org/10.1513/AnnalsATS.201407-320MG

62. Tschumperlin, D. J., Liu, F., & Tager, A. M. (2013). Biomechanical regulation of mesenchymal cell function. Current Opinion in Rheumatology, 25(1), 92–100. https://doi.org/10.1097/BOR.0b013e32835b13cd

63. White, L. J., Taylor, A. J., Faulk, D. M., Keane, T. J., Saldin, L. T., Reing, J. E., Swinehart, I. T., Turner, N. J., Ratner, B. D., & Badylak, S. F. (2017). The impact of detergents on the tissue decellularization process: a ToF-SIMS study. Acta Biomaterialia, 50, 207–219. https://doi.org/10.1016/j.actbio.2016.12.033

64. Wu, D., & Birukov, K. (2019). Endothelial Cell Mechano-Metabolomic Coupling to Disease States in the Lung Microvasculature. Frontiers in Bioengineering and Biotechnology, 7, 172. https://doi.org/10.3389/fbioe.2019.00172

65. Young, B. M., Shankar, K., Tho, C. K., Pellegrino, A. R., & Heise, R. L. (2019). Laminin-driven Epac/Rap1 regulation of epithelial barriers on decellularized matrix. Acta Biomaterialia, 100, 223–234. https://doi.org/10.1016/j.actbio.2019.10.009

66. Yue, B. (2014). Biology of the Extracellular Matrix: An Overview. Journal of Glaucoma, S20–S23. https://doi.org/10.1097/IJG.0000000000000108

67. Zhou, Y., Horowitz, J. C., Naba, A., Ambalavanan, N., Atabai, K., Balestrini, J., Bitterman, P. B., Corley, R. A., Ding, B.-S., Engler, A. J., Hansen, K. C., Hagood, J. S., Kheradmand, F., Lin, Q. S., Neptune, E., Niklason, L., Ortiz, L. A., Parks, W. C., Tschumperlin, D. J., … Thannickal, V. J. (2018). Extracellular matrix in lung development, homeostasis and disease. Matrix Biology, 73, 77–104. https://doi.org/10.1016/j.matbio.2018.03.005